

Error Analysis on a Novel Class of Exponential Integrators with Local Linear Extension Techniques for Highly Oscillatory ODEs

Zhihao Qi^a, Weibing Deng^{a,*}, Fuhai Zhu^a

^a*School of Mathematics, Nanjing University, Nanjing 210093, People's Republic of China*

Abstract

This paper studies a class of non-autonomous highly oscillatory ordinary differential equations (ODEs) featuring a linear component inversely proportional to a small parameter ε with purely imaginary eigenvalues, alongside an ε -independent nonlinear component. When $0 < \varepsilon \ll 1$, the rapidly oscillatory solution constrains the step size selection and numerical accuracy, resulting in significant computational challenges. Motivated by linearization through introducing auxiliary polynomial variables, a new class of explicit exponential integrators (EIs) has recently been developed. The methods do not require the linear part to be diagonal or with all eigenvalues to be integer multiples of a fixed value—a general assumption in multiscale methods—and attain arbitrarily high convergence order without any order conditions. The main contribution of this work is to establish a rigorous error analysis for the new class of methods. To do this, we first demonstrate the equivalence between the high-dimensional system and the original problem by employing algebraic techniques. Building upon these fundamental results, we prove that the numerical schemes have a uniform convergence order of $O(h^{k+1})$ for the solution when using at most k -degree auxiliary polynomial variables with time step sizes smaller than ε . For larger step sizes under the bounded oscillatory energy condition, the methods achieve a convergence order of $O(\varepsilon h^k)$ for the solution. These theoretical results are further applied to second-order oscillatory equations, yielding improved uniform accuracy with respect to ε . Finally, numerical experiments confirm the optimality of the derived error estimates.

Keywords: Local linearization, Highly oscillatory systems, Uniform accuracy, Exponential integrator, Variation-of-constants formula

*Corresponding author

Email addresses: zhihaoqi@smail.nju.edu.cn (Zhihao Qi), wbdeng@nju.edu.cn (Weibing Deng), zhufuhai@nju.edu.cn (Fuhai Zhu)

1. Introduction

In this work, we study the ODE systems with the form

$$\begin{aligned}\dot{\mathbf{u}} &= \frac{1}{\varepsilon} A\mathbf{u} + \mathbf{F}(\mathbf{u}, t), \quad t \in [0, T], \\ \mathbf{u}(0) &= \varepsilon^\nu \mathbf{u}_{\text{in}},\end{aligned}\tag{1.1}$$

where $\mathbf{u} \in \mathbb{C}^d$ ($d \geq 1$) represents the solution vector, ε is a dimensionless parameter characterizing the oscillation frequency, $\nu \in \mathbb{R}$ characterizes the scale of the initial value, $\mathbf{u}_{\text{in}} \in \mathbb{C}^d$ is a given vector, and $T > 0$ denotes the final time independent of ε . The matrix $A = (A_{ij})_{d \times d}$ is assumed to possess purely imaginary eigenvalues and is required to be diagonalizable, but not necessarily diagonal. The nonlinear forcing term \mathbf{F} is time-dependent and Lipschitz continuous in all variables with an ε -independent Lipschitz constant. For $0 < \varepsilon \ll 1$, system (1.1) describes a broad class of highly oscillatory problems driven dominantly by linear oscillators since the $O(\varepsilon^{-1})$ norm in the linear operator governs the oscillatory characteristics. The purely imaginary spectrum of matrix A indicates that each solution component has oscillatory behavior, propagating as a superposition of high-frequency waves with temporal wavelengths scaling as $O(\varepsilon)$. A typical problem is the second-order oscillatory equation [1, 2, 3, 4, 5, 6]

$$\begin{aligned}\ddot{\mathbf{y}} + \frac{1}{\varepsilon^2} M\mathbf{y} &= \mathbf{g}(\mathbf{y}, t), \quad t \in [0, T], \\ \mathbf{y}(0) &= \varepsilon^\nu \mathbf{y}_{\text{in}}, \quad \dot{\mathbf{y}}(0) = \varepsilon^{\nu-1} \dot{\mathbf{y}}_{\text{in}},\end{aligned}\tag{1.2}$$

where M is a symmetric positive-definite matrix and \mathbf{g} is a nonlinear function. This type of highly oscillatory system is ubiquitous in scientific computing, arising in many fields, including classical mechanics, molecular dynamics, quantum physics, astronomy, circuit simulation, and plasma physics [7, 8, 9, 5, 10]. We introduce the scaled momentum variable $\mathbf{p} = \varepsilon \dot{\mathbf{y}}$ and set $\mathbf{u} = [\mathbf{y}^\top, \mathbf{p}^\top]^\top$, then the system (1.2) is recast to (1.1). If the right-hand side \mathbf{g} of (1.2) is independent of t and there exists a potential function $U(\mathbf{y})$ satisfying $\mathbf{g}(\mathbf{y}) = -\nabla U(\mathbf{y})$, then (1.2) represents a Hamiltonian system [11]. The Hamiltonian takes the form

$$H(\mathbf{y}, \dot{\mathbf{y}}) = H_1(\mathbf{y}, \dot{\mathbf{y}}) + U(\mathbf{y})\tag{1.3}$$

with

$$H_1(\mathbf{y}, \dot{\mathbf{y}}) = \frac{1}{2} \|\dot{\mathbf{y}}\|^2 + \frac{1}{2\varepsilon^2} \mathbf{y}^\top M \mathbf{y},\tag{1.4}$$

where $\|\cdot\|$ denotes the standard Euclidean norm. The quantity (1.4) characterizes the total kinetic and potential energy associated with the linear oscillator component of (1.2). As an invariant, the Hamiltonian (1.3) satisfies $H(\mathbf{y}(t), \dot{\mathbf{y}}(t)) = H(\mathbf{y}(0), \dot{\mathbf{y}}(0))$ for all time $t > 0$. In highly oscillatory problems, H_1 dominates the total energy H . Such systems with bounded oscillatory energy are physically relevant in many applications, where H_1 admits an ε -independent upper bound, implying the parameter regime $\nu \geq 1$. More generally, the source on the right-hand side of (1.2) models both the internal forces within the system and time-dependent external interactions, making (1.2) applicable beyond the conservative system. Nevertheless, the definition of oscillatory energy (1.4) remains valid, and thus $\nu \geq 1$ can still be regarded as a necessary condition for bounding the oscillatory energy in (1.1).

From the view of computation, the highly oscillatory nature of the solution poses fundamental challenges for numerical treatment, rendering many classical numerical schemes inefficient or even ineffective. The overly large linear terms in (1.1) impose severe stability constraints on conventional numerical methods, including standard Runge-Kutta and Runge-Kutta-Nyström methods [12, 5]. To maintain numerical reliability, the time step size must resolve the highest oscillation frequency, requiring the restrictive condition $h < C\varepsilon$ [13, 14], where C represents a constant independent of both h and ε . The computation of repetitive circular motions brings substantial practical burdens and demands considerable computational resources, hence severely limiting practical efficiency. Moreover, when applied to (1.1), most conventional numerical methods exhibit increasing errors as the system frequency grows. These methods are constructed based on Taylor expansions of the exact solution whose remainders dominate truncation errors. Therefore, the global error typically depends on the negative powers of ε since the temporal derivatives of the solution scale of $1/\varepsilon^k$ for some $k > 0$ [15, 16]. In other words, these traditional approaches lack uniform accuracy with respect to ε , making them unsuitable for solving (1.1) when ε is arbitrarily small.

To address these numerical challenges, in the 1960s, Gautschi initially proposed the utilization of trigonometric polynomials to handle high-frequency components based on the variation-of-constants formula [17]. Later, various Gautschi-type trigonometric integrators were subsequently developed by the introduction of different filters [18, 19, 20]. The systematical investigation of the long-term behavior of numerical solutions employs the Modulated Fourier expansion technique introduced in [9], with related works in [21, 22, 23, 24, 25]. When system (1.1) represents highly oscillatory Hamiltonian dynamical systems [11], a wealth of research has been dedicated to designing structure-

preserving numerical solvers (see [9, 18, 20, 26, 14, 27, 28] and reference therein). This class of methods can obtain reliable numerical approximations to the exact solution after substantial time steps by preserving the inherent structure of the original oscillatory problem in an equivalent long-time dynamical sense. However, most of these methods remain strictly constrained by stability conditions.

To confront step size limitations, the exponential integrators have emerged as powerful tools for stiff differential equations. In recent decades, EIs have attracted extensive attention and undergone vigorous development. Numerous excellent studies have been conducted [29, 30, 31, 32, 33, 34], with a comprehensive review available in [35]. The construction of EIs exploits the variation-of-constants formula, which provides an exact treatment of linear components. Due to their superior stability properties [29], this approach is particularly advantageous for systems where stiffness is predominantly concentrated in the linear part. When applying the variation-of-constants formula to second-order systems (1.2), the matrix exponential manifests naturally as trigonometric functions [26]. This observation has inspired several methods, including ARKN methods [2], ERKN methods [26, 27], and Filon-type methods [36, 37]. Many of these methods additionally exhibit excellent structure-preserving properties. Developments have also combined EIs with linearization operations [38, 39, 40, 32], such as the Exponential Rosenbrock-type methods [41, 30, 42], yielding improved accuracy and efficiency while simplifying order conditions. However, whether linearization is employed or not, conventional EIs are designed under the assumption of temporal smoothness for solutions of stiff systems. This underlying assumption is typically violated in highly oscillatory systems, leading to a loss of uniform accuracy.

Over the past two decades, various multiscale methods with ε -independent step sizes and accuracy have been proposed. The primary strategy of these methods is to transform the original system into a formulation independent of oscillation by leveraging high-frequency characteristics, thereby enabling the design of numerical methods with uniform accuracy. The Heterogeneous Multiscale Method [43, 44, 45, 46, 47], Multi-Revolution Composition Method [48, 49] and Stroboscopic Averaging Method [50, 4, 51, 52] primarily focus on capturing the averaging effects over multiple periods. The development of Multiscale Time Integrators [14, 13, 53] and Multiscale Exponential Wave Integrators [54, 55, 56] is motivated by asymptotic expansions of exact solutions. The Nested Picard Iteration scheme [57, 16, 58] iteratively applies the variation-of-constants formulas. The Two-Scale Formulation method [25, 6, 59] treats high-frequency components as additional variables

for discretization. While achieving uniform accuracy, many of these methods require structural assumptions for the matrix A . Some requirements include that all eigenvalues be integer multiples of a fixed value corresponding to the principal frequency, or a diagonal form obtained by assuming directly or by preprocessing steps involving diagonalization and variable transformations. These assumptions serve to decouple the system's oscillatory modes, thereby effectively simplifying the dynamics dominated by single-frequency behavior, which brings fundamental convenience for the construction of multiscale methods.

In this study, we present a theoretical analysis of a novel class of exponential integrators based on local linear extension recently developed in [60]. Unlike the aforementioned multiscale methods that exploit the inherent high-frequency characteristics of the equations, the proposed method primarily employs a dimension-raising technique to achieve linearization. Numerical methods developed within the EI framework can effectively utilize the variation-of-constants formula, which provides an exact treatment of the linear component without requiring special structural assumptions on matrix A or nonlinear function \mathbf{F} . The proposed local linearization strategy addresses the critical challenge of achieving uniform accuracy when applying the conventional EIs to (1.1) in small step size case or under the bounded oscillatory energy condition. Furthermore, these new EIs circumvent the order condition, thereby theoretically enabling the systematic construction of arbitrarily high-order schemes. The numerical solution of (1.1) is obtained through the following computational framework. First, we introduce a set of auxiliary variables that depend on the numerical solutions \mathbf{u}_n at each time step t_n , taking the form of polynomial functions in \mathbf{u} up to degree k . Subsequently, we derive the governing equations for these auxiliary polynomial variables from the original system (1.1), thereby constructing an equivalent high-dimensional ODE system referred to as the local linear extension system. Numerical approximations \mathbf{u}_{n+1} of the exact solutions $\mathbf{u}(t_{n+1})$ at the next time step are then obtained by applying EIs to this extension system, followed by a projection operation that maps the high-dimensional solution back to the original state space. The key insight of this approach stems from the observation that, through dimension-raising transformation, the k -th order Taylor expansion of the nonlinear term \mathbf{F} depends linearly on the high-dimensional variable. Although the extension system maintains its highly oscillatory nature, the reconstructed linear part incorporates more information than its counterpart in the original system. The new EIs are fully explicit, not only ensuring computational efficiency but also allowing the achievement of uniform accuracy without requiring any iterative procedures.

The primary contribution of the current work lies in establishing a rigorous theoretical analysis for the novel EIIs. For small time steps satisfying $h < C\varepsilon$, the methods applied to (1.1) achieve uniform error bounds of $O(h^{k+1})$ for the solution, where k denotes the highest degree of the auxiliary polynomial variables. For systems with bounded oscillatory energy when using large time steps $h > C\varepsilon$, the methods can achieve a convergence order of $O(\varepsilon h^k)$. The analysis fundamentally relies on the application of adiabatic transformation [35, 61, 1] and period decomposition techniques, enabling the individual treatment of each oscillatory component within the high-dimensional system. It is particularly noteworthy to show the non-triviality of the fact that the $O(\frac{1}{\varepsilon})$ -scaled linear part in the high-dimensional system preserves the spectral property of A . We rigorously prove this preservation—playing a crucial role in the theoretical analysis for uniform accuracy—through careful algebraic derivation. A further analytical challenge lies in the potential resonance phenomena among high-frequency components in the high-dimensional system, where the periodic decomposition technique is ineffective for their analysis. To address this difficulty, we examine the invariant subspaces and their associated matrix representations corresponding to the $O(\frac{1}{\varepsilon})$ -scaled operators in high dimensions. This analytical framework successfully eliminates resonance effects from our error estimates. As a direct application, we extend the theoretical findings to the second-order system (1.2), deriving higher-order error estimates with improved uniform convergence.

The remainder of this paper is organized as follows. Section 2 reviews the construction of local linear extension exponential integrators. Section 3 is devoted to analyzing the algebraic properties of the linear part in the local linear extension system, while Section 4 presents the convergence analysis under various conditions. Several typical numerical experiments are conducted in Section 5 to validate the theoretical results. The last section concludes this paper.

2. The local linear extension exponential integrators

This section concisely reviews the construction methodology for the local linear extension system and the associated EIIs. We first treat time t as an independent variable and define the augmented state vector $\mathbf{x} = [\mathbf{u}^\top, t]^\top$. The original system (1.1) is reformulated as

$$\begin{aligned}\dot{\mathbf{x}} &= \frac{1}{\varepsilon} A_1 \mathbf{x} + \mathbf{f}(\mathbf{x}), \\ \mathbf{x}(0) &= \varepsilon^\nu \mathbf{x}_{\text{in}},\end{aligned}\tag{2.1}$$

where

$$A_1 = (A_1)_{ij} = \begin{bmatrix} A & \mathbf{0}_{d_1 \times 1} \\ \mathbf{0}_{1 \times d_2} & 0 \end{bmatrix}, \quad \mathbf{f}(\mathbf{x}) = \begin{bmatrix} \mathbf{F}(\mathbf{u}, t) \\ 1 \end{bmatrix}, \quad \mathbf{x}_{\text{in}} = \begin{bmatrix} \mathbf{u}_{\text{in}} \\ 0 \end{bmatrix}. \quad (2.2)$$

Here $\mathbf{0}_{d_1 \times d_2}$ represents a $d_1 \times d_2$ zero matrix.

Introducing local linear extension variables requires the preliminary definition of multi-indices and index sets with associated algebraic structures. For positive integers k and d , we define the index set as $\mathcal{I}_{d+1}^{[[k]]} := \{1, \dots, d+1\}^k$, the k -fold Cartesian product of the set $\{1, \dots, d+1\}$. Each element $\alpha \in \mathcal{I}_{d+1}^{[[k]]}$ represents a multi-index of length k , denoted by $|\alpha| = k$. Conventionally, for $k = 0$, we define $\mathcal{I}_{d+1}^{[[0]]}$ as the singleton set containing only the empty index with no components. We introduce the following equivalence relation on this index set $\mathcal{I}_{d+1}^{[[k]]}$.

Definition 2.1. (i) Let S_k denote the symmetric group on k elements. The right action of group S_k on the index set $\mathcal{I}_{d+1}^{[[k]]}$ is defined as follows: for any permutation $\sigma \in S_k$ of $\{1, \dots, k\}$ and multi-index $\alpha = (\alpha_1, \dots, \alpha_k) \in \mathcal{I}_{d+1}^{[[k]]}$,

$$\sigma(\alpha) := (\alpha_{\sigma(1)}, \dots, \alpha_{\sigma(k)}) \in \mathcal{I}_{d+1}^{[[k]]}.$$

(ii) Define an equivalence relation \sim on $\mathcal{I}_{d+1}^{[[k]]}$ induced by the group action: for any $\alpha, \beta \in \mathcal{I}_{d+1}^{[[k]]}$,

$$\alpha \sim \beta \iff \text{there exists } \sigma \in S_k \text{ such that } \sigma(\alpha) = \beta.$$

The equivalence follows immediately from the group properties of S_k . We denote by $[\alpha]$ the equivalence class containing α .

By arranging the components of each multi-index in ascending order, the subset of $\mathcal{I}_{d+1}^{[[k]]}$

$$\tilde{\mathcal{I}}_{d+1}^{[[k]]} := \{\alpha = (\alpha_1, \dots, \alpha_k) \in \mathcal{I}_{d+1}^{[[k]]} : \alpha_1 \leq \dots \leq \alpha_k\} \quad (2.3)$$

provides a natural choice of representative elements for each equivalence class. Although our subsequent construction of numerical schemes and analysis is independent of the choice of representatives, we fix the representatives to be those multi-indices having the form specified in (2.3) for convenience. For $\alpha \in \mathcal{I}_{d+1}^{[[k]]}$, we denote such representative multi-indices of $[\alpha]$ with form (2.3) by $\bar{\alpha}$. These preparations lead to the definition of local linear extension variables.

Definition 2.2. (i) We denote $\mathcal{I}_{d+1}^{[k]} := \bigcup_{j=0}^k \mathcal{I}_{d+1}^{[[j]]}$. For given $\hat{\mathbf{x}} = [\hat{\mathbf{u}}^\top, \hat{t}]^\top$ with $\hat{\mathbf{u}} \in \mathbb{C}^d$ and $\hat{t} \geq 0$, the polynomials induced by the multi-index $\alpha \in \mathcal{I}_{d+1}^{[k]}$ are given by

$$(\mathbf{x} - \hat{\mathbf{x}})^\alpha := \begin{cases} 1, & \text{if } |\alpha| = 0, \\ (x_{\alpha_1} - \hat{x}_{\alpha_1}) \cdots (x_{\alpha_j} - \hat{x}_{\alpha_j}), & \text{if } |\alpha| = j \geq 1, \end{cases} \quad (2.4)$$

where x_i and \hat{x}_i represent the i -th component of \mathbf{x} and $\hat{\mathbf{x}}$, respectively.

(ii) Denote the sets of polynomials of j -degree and no more than k -th degree in variable \mathbf{x} with the form (2.4) by

$$P_{\mathbf{x}}^{[[j, \hat{\mathbf{x}}]]} = \left\{ (\mathbf{x} - \hat{\mathbf{x}})^{\bar{\alpha}} : \bar{\alpha} \in \tilde{\mathcal{I}}_{d+1}^{[[j]]} \right\}, \quad P_{\mathbf{x}}^{[k, \hat{\mathbf{x}}]} = \bigcup_{j=0}^k P_{\mathbf{x}}^{[[j, \hat{\mathbf{x}}]]}. \quad (2.5)$$

respectively. Let $|\cdot|$ denote the cardinality for finite sets and let $D^{[k]} = |P_{\mathbf{x}}^{[k, \hat{\mathbf{x}}]}|$. We define a $D^{[k]}$ -dimensional vector, whose first component is 1, the second to the $(d+2)$ -th components correspond to $\mathbf{x} - \hat{\mathbf{x}}$, and the remaining components may be arranged in any prescribed order. This vector, denoted by $\mathbf{x}^{[k, \hat{\mathbf{x}}]}$, is referred to as the k -th order local linear extension variable at $\hat{\mathbf{x}}$. Furthermore, we introduce the $D^{[[j]]}$ -dimensional vectors $\mathbf{x}^{[[j, \hat{\mathbf{x}}]]}$ for $j = 0, \dots, k$, where $D^{[[j]]} = |P_{\mathbf{x}}^{[[j, \hat{\mathbf{x}}]]}|$, representing vectors composed of j -th degree polynomial components uniquely from $P_{\mathbf{x}}^{[[j, \hat{\mathbf{x}}]]}$. We introduce the projection operator extracting components m_1 through m_2 of a vector:

$$\Pi_{m_1}^{m_2} = [\mathbf{0}_{m \times (m_1-1)}, I_m, \mathbf{0}_{m \times (D^{[k]}-m_2)}], \quad \text{with } m = m_2 - m_1 + 1,$$

where I_m denotes the $m \times m$ identity matrix. Then we specify $\mathbf{x}^{[[0, \hat{\mathbf{x}}]]} = \Pi_1^1 \mathbf{x}^{[k, \hat{\mathbf{x}}]} = 1$ and $\mathbf{x}^{[[1, \hat{\mathbf{x}}]]} = \Pi_2^{d+2} \mathbf{x}^{[k, \hat{\mathbf{x}}]} = \mathbf{x} - \hat{\mathbf{x}}$.

(iii) The partial differential operator induced by the multi-index $\alpha \in \mathcal{I}_{d+1}^{[k]}$ is defined as

$$\frac{\partial^\alpha}{\partial \mathbf{x}^\alpha} := \begin{cases} \text{id}, & \text{if } |\alpha| = 0, \\ \frac{\partial^j}{\partial x_{\alpha_1} \cdots \partial x_{\alpha_j}}, & \text{if } |\alpha| = j \geq 1. \end{cases}$$

Remark 2.3. Any valid sorting scheme is permitted for the components excluding the first $(d+2)$ -th of $\mathbf{x}^{[k, \hat{\mathbf{x}}]}$, as different choices lead to equivalent numerical schemes and theoretical analyses. For example, the study in [60] chooses the sorting scheme

$$\mathbf{x}^{[k, \hat{\mathbf{x}}]} = \left[\mathbf{x}^{[[0, \hat{\mathbf{x}}]]} \quad (\mathbf{x}^{[[1, \hat{\mathbf{x}}]]})^\top \quad \dots \quad (\mathbf{x}^{[[k, \hat{\mathbf{x}}]]})^\top \right]^\top. \quad (2.6)$$

The standard lexicographical order is applied to the multi-indices in $\mathcal{I}_{d+1}^{[[j]]}$ ($j = 2, \dots, k$), which uniquely specify a sorting for the components of $\mathbf{x}^{[[j, \hat{\mathbf{x}}]]}$ through (2.4).

By Definition 2.2, the set $P_{\mathbf{x}}^{[k, \hat{\mathbf{x}}]}$ forms a basis spanning the space of polynomials of degree at most k in variables x_1, \dots, x_{d+1} , denoted by $\mathbb{P}^k[\mathbf{x}]$. Employing the partial derivatives and polynomials in Definition 2.2, we derive the k -th order Taylor expansion of \mathbf{f} about a reference point $\hat{\mathbf{x}}$

$$\mathbf{f}(\mathbf{x}) = \sum_{j=0}^k \sum_{\bar{\alpha} \in \tilde{\mathcal{I}}_{d+1}^{[j]}} \frac{1}{\gamma(\bar{\alpha})} \frac{\partial^{\bar{\alpha}} \mathbf{f}(\hat{\mathbf{x}})}{\partial \mathbf{x}^{\bar{\alpha}}} (\mathbf{x} - \hat{\mathbf{x}})^{\bar{\alpha}} + \bar{\mathbf{r}}^{k+1}(\mathbf{x}; \hat{\mathbf{x}}), \quad (2.7)$$

where $\gamma(\alpha) = \prod_{q=1}^{d+1} |\alpha_{\{q\}}|!$ with the set $\alpha_{\{q\}} = \{j : \alpha_j = q\}$ representing components of the multi-index α with their value q . The term $\bar{\mathbf{r}}^{k+1}(\mathbf{x}; \hat{\mathbf{x}})$ denotes the $(k+1)$ -th order Taylor remainder. According to (2.2), we have

$$\bar{\mathbf{r}}^{k+1}(\mathbf{x}; \hat{\mathbf{x}}) := \begin{bmatrix} \mathbf{r}^{k+1}(\mathbf{u}, t; \hat{\mathbf{u}}, \hat{t}) \\ 0 \end{bmatrix}, \quad (2.8)$$

where $\mathbf{r}^{k+1}(\mathbf{u}, t; \hat{\mathbf{u}}, \hat{t})$ denotes the $(k+1)$ -th order Taylor remainder of $\mathbf{F}(\mathbf{u}, t)$ expanded at $(\hat{\mathbf{u}}, \hat{t})$. As the variables in $P_{\mathbf{x}}^{[k, \hat{\mathbf{x}}]}$ remain unknown, we now derive the governing equations for these auxiliary polynomial variables to close the system. Consider a reference point $\hat{\mathbf{x}}$ and a multi-index $\alpha \in \mathcal{I}_{d+1}^{[k]}$ with its length j . Exploiting (2.1) and (2.4), we obtain

$$\begin{aligned} \frac{d}{dt}(\mathbf{x} - \hat{\mathbf{x}})^\alpha &= \sum_{l=1}^j \frac{(x_{\alpha_1} - \hat{x}_{\alpha_1}) \cdots (x_{\alpha_j} - \hat{x}_{\alpha_j})}{x_{\alpha_l} - \hat{x}_{\alpha_l}} \frac{d(x_{\alpha_l} - \hat{x}_{\alpha_l})}{dt} \\ &= \sum_{l=1}^j (\mathbf{x} - \hat{\mathbf{x}})^{\chi(\alpha; l)} \left(\frac{1}{\varepsilon} \sum_{m=1}^{d+1} (A_1)_{\alpha_l m} x_m + f_{\alpha_l}(\mathbf{x}) \right) \\ &= \frac{1}{\varepsilon} \sum_{l=1}^j \sum_{m=1}^{d+1} (A_1)_{\alpha_l m} (\mathbf{x} - \hat{\mathbf{x}})^{\chi(\alpha; l)} (x_m - \hat{x}_m) + \frac{1}{\varepsilon} \sum_{l=1}^j \sum_{m=1}^{d+1} (A_1)_{\alpha_l m} \hat{x}_m (\mathbf{x} - \hat{\mathbf{x}})^{\chi(\alpha; l)} \\ &\quad + \sum_{l=1}^j \sum_{m=0}^{k-j+1} \sum_{\bar{\beta} \in \tilde{\mathcal{I}}_{d+1}^{[m]}} \frac{1}{\gamma(\bar{\beta})} \frac{\partial^{\bar{\beta}} \mathbf{f}(\hat{\mathbf{x}})}{\partial \mathbf{x}^{\bar{\beta}}} (\mathbf{x} - \hat{\mathbf{x}})^{\chi(\alpha; l)} (\mathbf{x} - \hat{\mathbf{x}})^{\bar{\beta}} + \sum_{l=1}^j (\mathbf{x} - \hat{\mathbf{x}})^{\chi(\alpha; l)} \bar{r}_{\alpha_l}^{k-j+2}(\mathbf{x}; \hat{\mathbf{x}}), \end{aligned} \quad (2.9)$$

where $\chi(\alpha; l) = (\alpha_1, \dots, \alpha_{l-1}, \alpha_{l+1}, \dots, \alpha_j) \in \mathcal{I}_{d+1}^{[[j-1]]}$ represents the multi-index formed by removing the l -th component from α . The final equality in (2.9) employs a $(k-j+1)$ -th order Taylor expansion of f_{α_l} , with f_{α_l} and $\bar{r}_{\alpha_l}^i$ representing the α_l -th components of the vector-valued functions \mathbf{f} and $\bar{\mathbf{r}}^i$, respectively.

A key observation reveals that all terms in (2.9) have the expression as linear combinations of polynomials from $P_{\mathbf{x}}^{[k, \hat{\mathbf{x}}]}$, except those involving the nonlinear remainders $\bar{r}_{\alpha_l}^{k-j+2}(\mathbf{x}; \hat{\mathbf{x}})$. We sum the

coefficients to consolidate identical polynomials, organised according to a specific ordering scheme, enabling representation of all terms in (2.9) (excluding the remainder term) as inner products of coefficient vectors and $\mathbf{x}^{[k,\hat{\mathbf{x}}]}$. Through differentiation of each polynomial component in $\mathbf{x}^{[k,\hat{\mathbf{x}}]}$ by (2.9), we aggregate the resulting coefficient vectors and isolate $O(\frac{1}{\varepsilon})$ terms from $O(1)$ components by the distinct scale. This process yields the coefficient matrices $A_1^{[k]}(\hat{\mathbf{x}})$ and $A_0^{[k]}(\hat{\mathbf{x}})$, thereby deriving the governing equation for the local linear extension variables $\mathbf{x}^{[k,\hat{\mathbf{x}}]}$:

$$\frac{d\mathbf{x}^{[k,\hat{\mathbf{x}}]}}{dt} = \frac{1}{\varepsilon} A_1^{[k]}(\hat{\mathbf{x}}) \mathbf{x}^{[k,\hat{\mathbf{x}}]} + A_0^{[k]}(\hat{\mathbf{x}}) \mathbf{x}^{[k,\hat{\mathbf{x}}]} + \mathbf{R}^{[k]}(\mathbf{x}^{[k,\hat{\mathbf{x}}]}; \hat{\mathbf{x}}). \quad (2.10)$$

Noting that there are no simple closed-form expressions for the matrices $A_1^{[k]}$ and $A_0^{[k]}$ in the compact formulation, we give a feasible algorithm to construct these matrices as follows. The primary methodology involves an element-wise process that assigns specific values to their respective positions. Specifically, we first get the row index of the matrices by traversing all multi-indices in $P_{\mathbf{x}}^{[k,\hat{\mathbf{x}}]}$. When treating the equation induced by a certain multi-index, we locate the column indices for the associated polynomials on the right-hand side of (2.9), followed by assigning the coefficients in (2.9) to this specific position. We refer to Algorithm 1 in [60] for implementing details.

The explicit formulation of the remainder term $\mathbf{R}^{[k]}$ is crucial for analytical purposes. Let the i -th row of (2.10) correspond to the equation generated by the multi-index α . Since the $(d+1)$ -th row in (2.8) is zero, the i -th component of $\mathbf{R}^{[k]}(\mathbf{x}^{[k,\hat{\mathbf{x}}]}; \hat{\mathbf{x}})$ is given by

$$R_i^{[k]}(\mathbf{x}^{[k,\hat{\mathbf{x}}]}; \hat{\mathbf{x}}) = \sum_{l=1}^j \sum_{\alpha_l \neq d+1} (\mathbf{x} - \hat{\mathbf{x}})^{\chi(\alpha;l)} r_{\alpha_l}^{k-j+2}(\mathbf{u}, t; \hat{\mathbf{u}}, \hat{t}). \quad (2.11)$$

Then we have the following definition of local linear extension system.

Definition 2.4. For a given reference point $\hat{\mathbf{x}}$ and positive integer k , let $\mathbf{x}^{[k,\hat{\mathbf{x}}]}$ denote the k -th order local linear extension variable at $\hat{\mathbf{x}}$. We refer to the above procedure to generate system (2.10) as the local linear extension operations, and define (2.10) as the k -th order local linear extension system of (2.1) at $\hat{\mathbf{x}}$.

When constructing the local linear extension system, our approach employs the Taylor expansion of $\mathbf{f}(\mathbf{x})$ with respect to \mathbf{x} in (2.9), rather than expanding $\mathbf{f}(\mathbf{x}(t))$ solely in t where conventional EIs are conceptually based. This critical distinction ensures the linear component of (2.10) incorporates enhanced information than (2.1), while the resulting formulation maintains ε -independence, which is essential for designing uniformly accurate methods.

To obtain a numerical solution for system (2.1), we discretize the time interval $[0, T]$ by employing uniform steps, denoted as $0 = t_0 < t_1 < \dots < t_N = T$, with a constant step size $h = t_n - t_{n-1}$, where $n = 1, \dots, N$. We now develop the numerical methods for solving (2.1) based on the local linear extension system (2.10). Let \mathbf{X}_n represent the numerical solution to $\mathbf{x}(t_n)$. Taking $\hat{\mathbf{x}} = \mathbf{X}_n$ as the reference point in Definition 2.2, we construct the k -th order local linear extension variable $\mathbf{X}^{[k, \mathbf{X}_n]}$ associated with the numerical solution. As indicated in Definition 2.2, evaluation at time t_n yields $\mathbf{X}^{[k, \mathbf{X}_n]}(t_n) = e_1$, where e_j denotes the j -th canonical basis vector. We define the initial value problem satisfied by the extension variable $\mathbf{X}^{[k, \mathbf{X}_n]}(t)$ over the interval $[t_n, t_{n+1}]$ as

$$\begin{aligned} \frac{d\mathbf{X}^{[k, \mathbf{X}_n]}}{dt} &= \frac{1}{\varepsilon} A_1^{[k]}(\mathbf{X}_n) \mathbf{X}^{[k, \mathbf{X}_n]} + A_0^{[k]}(\mathbf{X}_n) \mathbf{X}^{[k, \mathbf{X}_n]}, \quad t_n \leq t \leq t_{n+1}, \\ \mathbf{X}^{[k, \mathbf{X}_n]}(t_n) &= e_1, \end{aligned} \quad (2.12)$$

which represents a linear truncation of (2.10), obtained by setting the reference point $\hat{\mathbf{x}} = \mathbf{X}_n$ and neglecting the remainder term $\mathbf{R}^{[k]}$. Its exact solution provides $\mathbf{X}^{[k, \mathbf{X}_n]}(t)$ at the next time step

$$\mathbf{X}^{[k, \mathbf{X}_n]}(t_{n+1}) = e^{\left(\frac{1}{\varepsilon} A_1^{[k]}(\mathbf{X}_n) + A_0^{[k]}(\mathbf{X}_n)\right)h} e_1. \quad (2.13)$$

Following Definition 2.2, we recover the numerical solution of (2.1) at t_{n+1} through the projection

$$\mathbf{X}_{n+1} := \Pi_2^{d+1} \mathbf{X}^{[k, \mathbf{X}_n]}(t_{n+1}) + \mathbf{X}_n. \quad (2.14)$$

The equivalence between (2.1) and (1.1) leads to the numerical solution for $\mathbf{u}(t_{n+1})$ as

$$\mathbf{U}_{n+1} := \Pi_1^d \mathbf{X}_{n+1}. \quad (2.15)$$

The resulting scheme (2.13)-(2.15) is fully explicit and requires no iterative procedures. The analysis in Section 4 demonstrates that these integrators achieve a convergence order of $k+1$ with respect to h when employing k -th order extension variables, implying that the improved convergence order stems directly from augmenting the dimensionality of the matrices $A_1^{[k]}$ and $A_0^{[k]}$. That is to say, these EIs can theoretically achieve an arbitrary high-order accuracy without requiring order conditions.

3. Algebraic properties of $A_1^{[k]}$

3.1. Linear extension lemma

When implementing EIs, the properties of the linear part in (2.12), predominantly governed by $A_1^{[k]}(\hat{\mathbf{x}})$, fundamentally determine the performance of the numerical scheme. While all eigenvalues

of A_1 have zero real parts, it is natural to examine whether $A_1^{[k]}(\hat{\mathbf{x}})$ generated through local linear extension operations preserve this property. The introduction of spurious eigenvalues with positive real parts - not inherent to the original problem - would significantly complicate the dynamics of the high-dimensional extension system. Fortunately, the following lemma precludes this case.

Lemma 3.1. *Suppose the local linear extension operation acting on (2.1) gives $A_1^{[k]}(\hat{\mathbf{x}})$ with A_1 defined in (2.2). Then $A_1^{[k]}(\hat{\mathbf{x}})$ is diagonalizable with all eigenvalues having zero real parts.*

Since the matrix $A_1^{[k]}(\hat{\mathbf{x}})$ is intrinsically determined only by the linear $O(\frac{1}{\varepsilon})$ component in (2.1), we define the operator D_1 by

$$D_1(\mathbf{x}) = \lim_{\varepsilon \rightarrow 0^+} \varepsilon \frac{d\mathbf{x}(t)}{dt}. \quad (3.1)$$

Applying D_1 to (2.1) and (2.10) respectively yields

$$D_1(\mathbf{x}) = A_1 \mathbf{x}, \quad (3.2)$$

$$D_1(\mathbf{x}^{[k, \hat{\mathbf{x}}]}) = A_1^{[k]}(\hat{\mathbf{x}}) \mathbf{x}^{[k, \hat{\mathbf{x}}]}. \quad (3.3)$$

We first present the structure of $A_1^{[k]}(\hat{\mathbf{x}})$ through two lemmas.

Lemma 3.2. *Suppose the ordering scheme for the extension variables is defined by (2.6). The matrix $A_1^{[k]}(\hat{\mathbf{x}})$ has the block bidiagonal structure*

$$A_1^{[k]}(\hat{\mathbf{x}}) = \begin{bmatrix} 0 & & & & \\ B_1^{[[1]]}(\hat{\mathbf{x}}) & A_1^{[[1]]} & & & \\ \ddots & \ddots & \ddots & & \\ & B_1^{[[k]]}(\hat{\mathbf{x}}) & A_1^{[[k]]} & & \end{bmatrix}, \quad (3.4)$$

where $A_1^{[[j]]}$ and $B_1^{[[j]]}(\hat{\mathbf{x}})$ ($j = 1, \dots, k$) are matrices of size $D^{[[j]]} \times D^{[[j]]}$ and $D^{[[j]]} \times D^{[[j-1]]}$, respectively. In particular, $A_1^{[[1]]} = A_1$.

Proof. Using (3.1) and (3.2), we can verify that the operator D_1 satisfies the Leibniz rule, i.e.,

$$D_1((x_i - \hat{x}_i)(x_j - \hat{x}_j)) = D_1(x_i - \hat{x}_i)(x_j - \hat{x}_j) + (x_i - \hat{x}_i)D_1(x_j - \hat{x}_j), \quad i, j \in \mathcal{I}_{d+1}^{[[1]]}. \quad (3.5)$$

Then for any multi-index $\alpha \in \mathcal{I}_{d+1}^{[[k]]}$ ($k \geq 1$), noticing (2.4), we have

$$\begin{aligned}
D_1((\mathbf{x} - \hat{\mathbf{x}})^\alpha) &= \sum_{j=1}^k (\mathbf{x}_{\alpha_1} - \hat{\mathbf{x}}_{\alpha_1}) \cdots D_1(\mathbf{x}_{\alpha_j} - \hat{\mathbf{x}}_{\alpha_j}) \cdots (\mathbf{x}_{\alpha_k} - \hat{\mathbf{x}}_{\alpha_k}) \\
&= \sum_{j=1}^k (\mathbf{x}_{\alpha_1} - \hat{\mathbf{x}}_{\alpha_1}) \cdots \left(\sum_{l=1}^{d+1} (A_1)_{\alpha_j l} \mathbf{x}_l \right) \cdots (\mathbf{x}_{\alpha_k} - \hat{\mathbf{x}}_{\alpha_k}) \\
&= \sum_{j=1}^k \sum_{l=1}^{d+1} (A_1)_{\alpha_j l} (\mathbf{x}_{\alpha_1} - \hat{\mathbf{x}}_{\alpha_1}) \cdots (\mathbf{x}_l - \hat{\mathbf{x}}_l) \cdots (\mathbf{x}_{\alpha_k} - \hat{\mathbf{x}}_{\alpha_k}) \\
&\quad + \sum_{j=1}^k \sum_{l=1}^{d+1} (A_1)_{\alpha_j l} \hat{\mathbf{x}}_l \frac{(\mathbf{x}_{\alpha_1} - \hat{\mathbf{x}}_{\alpha_1}) \cdots (\mathbf{x}_{\alpha_k} - \hat{\mathbf{x}}_{\alpha_k})}{\mathbf{x}_{\alpha_j} - \hat{\mathbf{x}}_{\alpha_j}}. \tag{3.6}
\end{aligned}$$

The first double summation in (3.6) corresponds to a k -th degree polynomial, while the second one represents a $(k-1)$ -th degree polynomial. This fact determines the unique matrices $A_1^{[[k]]} \in \mathbb{C}^{D^{[[k]]} \times D^{[[k]]}}$ and $B_1^{[[k]]}(\hat{\mathbf{x}}) \in \mathbb{C}^{D^{[[k]]} \times D^{[[k-1]]}}$ satisfying

$$D_1(\mathbf{x}^{[[k, \hat{\mathbf{x}}]]}) = A_1^{[[k]]} \mathbf{x}^{[[k, \hat{\mathbf{x}}]]} + B_1^{[[k]]}(\hat{\mathbf{x}}) \mathbf{x}^{[[k-1, \hat{\mathbf{x}}]]}.$$

The case $k = 0$ corresponds directly to a row of all zeros in $A_1^{[k]}(\hat{\mathbf{x}})$. Therefore, $A_1^{[k]}(\hat{\mathbf{x}})$ possesses the structure (3.4) \square

Lemma 3.3. *Suppose the ordering scheme for the extension variables is defined by (2.6). Then the following properties of $A_1^{[k]}(\hat{\mathbf{x}})$ hold:*

- (i) All matrices $A_1^{[k]}(\hat{\mathbf{x}})$ generated with different reference points $\hat{\mathbf{x}}$ are similar.
- (ii) There exists an invertible lower triangular matrix $S^{[k]}(\hat{\mathbf{x}})$, whose entries and those of its inverse are polynomials in $\hat{\mathbf{x}}$, such that $A_1^{[k]}(\mathbf{0}_{(d+1) \times 1}) = (S^{[k]}(\hat{\mathbf{x}}))^{-1} A_1^{[k]}(\hat{\mathbf{x}}) S^{[k]}(\hat{\mathbf{x}})$. Moreover, $S^{[k]}(\hat{\mathbf{x}})$ exhibits a nested block structure

$$S^{[1]}(\hat{\mathbf{x}}) = \begin{bmatrix} 1 \\ -\hat{\mathbf{x}} & I_{d+1} \end{bmatrix}, \quad S^{[k]}(\hat{\mathbf{x}}) = \begin{bmatrix} S^{[k-1]}(\hat{\mathbf{x}}) \\ * & I_{D^{[[k]]}} \end{bmatrix}. \tag{3.7}$$

Proof. For (i), we note that the components in local linear extension variables with different choices of reference point $\hat{\mathbf{x}}$ in Definition 2.2 span the same polynomial space. Therefore, the matrices $A_1^{[k]}(\hat{\mathbf{x}})$ derived from the action of D_1 on $P_{\mathbf{x}}^{[k, \hat{\mathbf{x}}]}$ with different $\hat{\mathbf{x}}$ exhibit the similarity relation.

For (ii), it suffices to examine the transition matrix from the basis $P_{\mathbf{x}}^{[k, \mathbf{0}]}$ to $P_{\mathbf{x}}^{[k, \hat{\mathbf{x}}]}$ and take it as $S^{[k]}(\hat{\mathbf{x}})$. It can be directly verified that $\mathbf{x}^{[1, \hat{\mathbf{x}}]} = S^{[1]}(\hat{\mathbf{x}}) \mathbf{x}^{[1, \mathbf{0}]}$, where $S^{[1]}(\hat{\mathbf{x}})$ is defined as in (3.7). For

any polynomial in $P_{\mathbf{x}}^{[k, \hat{\mathbf{x}}]}$ of the form (2.4), its expansion in terms of monomials from $P_{\mathbf{x}}^{[k, \mathbf{0}]}$ yields coefficients that are polynomials in $\hat{\mathbf{x}}$. It follows that all entries of $S^{[k]}(\hat{\mathbf{x}})$ are also polynomials in $\hat{\mathbf{x}}$. Since the coefficient of the highest-degree term in each polynomial is 1, the monomial expansion implies that the lower-right block of $S^{[k]}(\hat{\mathbf{x}})$ is the identity matrix $I_{D^{[[k]]}}$ under the ordering scheme (2.6). The nested structure (3.7) also follows immediately from (2.6). Moreover, the block structure of $S^{[k]}(\hat{\mathbf{x}})$ allows direct computation of its inverse. By induction, all entries of this inverse matrix are also polynomials in $\hat{\mathbf{x}}$. \square

The conclusion (i) in Lemma 3.3 ensures the identical spectral characteristics and diagonalizability for all $A_1^{[k]}(\hat{\mathbf{x}})$ with different $\hat{\mathbf{x}}$. Without loss of generality, we adopt $\hat{\mathbf{x}} = \mathbf{0}_{(d+1) \times 1}$ in subsequent derivations. Then through (3.6), all $B_1^{[[j]]}(\mathbf{0})(j = 1, \dots, k)$ are reduced to zero matrices, leading to the simplification of (3.4) to the block diagonal form

$$A_1^{[k]}(\mathbf{0}) = \text{diag}\{0, A_1^{[[1]]}, \dots, A_1^{[[k]]}\}, \quad (3.8)$$

and the following system of linear equations for $\mathbf{x}^{[[j, \mathbf{0}]]}$

$$D_1(\mathbf{x}^{[[j, \mathbf{0}]]}) = A_1^{[[j]]} \mathbf{x}^{[[j, \mathbf{0}]]}, \quad j = 1, \dots, k. \quad (3.9)$$

To analyze the eigenvalues and diagonalizability of $A_1^{[k]}(\hat{\mathbf{x}})$, it is sufficient to study these properties on the blocks $A_1^{[[j]]}(j = 1, \dots, k)$. However, the traditional analytical methods based on characteristic polynomials and eigenspace decomposition are unavailable due to the lack of explicit formulation of the matrices $A_1^{[[j]]}$. To circumvent this difficulty, we adopt an alternative strategy as follows. The main framework is to examine a higher-dimensional linear space, equipped with two distinct basis sets. The first basis yields a matrix representation of D_1 with a simple structure constructed via tensor products (see Lemma 3.4 below). This representation satisfies the spectral and diagonalizability properties asserted in Lemma 3.1 (see Lemma 3.5 below). For the second basis, the corresponding matrix representation contains the target matrices $A_1^{[[j]]}$ as subblocks (see Lemma 3.6 below). The similarity relation connecting these two matrix representations ensures that the desired spectral properties extend directly to $A_1^{[[j]]}$.

Let $V = \mathbb{P}^1[\mathbf{x}] / \mathbb{P}^0[\mathbf{x}]$ denote the quotient space formed by the space of complex polynomials of degree at most one with $d+1$ variables modulo the constant polynomials. The space V is naturally isomorphic to $\{\sum_{j=1}^{d+1} c_j x_j, c_j \in \mathbb{C}\}$, and we shall not distinguish between these two isomorphic spaces hereafter. Consequently, we regard $P_{\mathbf{x}}^{[[1, \mathbf{0}]]} \subset V$ as a basis for V . (3.2) induces a linear

mapping of D_1 , whose matrix representation relative to basis $P_{\mathbf{x}}^{[[1,0]]}$ is A_1 . Finally, we denote by $V^k = V^{\otimes k}$ the k -fold tensor product space of V .

Lemma 3.4. *D_1 can be extended to a linear mapping on the tensor product space V^k . We define*

$$\widehat{\mathcal{A}}_j^{[[k]]} = I_{d+1}^{\otimes(j-1)} \otimes A_1 \otimes I_{d+1}^{\otimes(k-j)}, \quad j = 1, \dots, k,$$

where the superscript \otimes^i denotes the i -fold tensor product operation. Then the matrix representation of D_1 relative to the tensor product basis $\{x_{\alpha_1} \otimes \dots \otimes x_{\alpha_k} : \alpha \in \mathcal{I}_{d+1}^{[[k]]}\}$ is given by

$$\mathcal{A}^{[[k]]} = \sum_{j=1}^k \widehat{\mathcal{A}}_j^{[[k]]}. \quad (3.10)$$

Proof. Given any tensor $\eta = \eta_1 \otimes \dots \otimes \eta_k \in V^k$, the Leibniz rule (3.5) yields

$$D_1(\eta_1 \cdot \eta_2 \cdots \eta_k) = \sum_{j=1}^k \eta_1 \cdots \eta_{j-1} \cdot D_1(\eta_j) \cdot \eta_{j+1} \cdots \eta_k.$$

One can directly define the action of $D_1 : V^k \rightarrow V^k$

$$D_1(\eta_1 \otimes \dots \otimes \eta_k) = \sum_{j=1}^k \eta_1 \otimes \dots \otimes \eta_{j-1} \otimes D_1(\eta_j) \otimes \eta_{j+1} \otimes \dots \otimes \eta_k. \quad (3.11)$$

The linearity follows immediately. If the tensor η is chosen within the basis set $\{x_{\alpha_1} \otimes \dots \otimes x_{\alpha_k} : \alpha \in \mathcal{I}_{d+1}^{[[k]]}\}$, a direct computation applying (3.2) and (3.11) yields

$$D_1(x_{\alpha_1} \otimes \dots \otimes x_{\alpha_k}) = \sum_{j=1}^k \sum_{l=1}^{d+1} (A_1)_{\alpha_j l} x_{\alpha_1} \otimes \dots \otimes x_{\alpha_{j-1}} \otimes x_l \otimes x_{\alpha_{j+1}} \otimes \dots \otimes x_{\alpha_k},$$

which gives the matrix representation (3.10). \square

Lemma 3.5. *Let $\lambda(A_1) = \{\lambda_1, \dots, \lambda_{d+1}\} \subset \mathbb{C}$ denote the spectrum of A_1 . Then the spectrum of $\mathcal{A}^{[[k]]}$ satisfies $\lambda(\mathcal{A}^{[[k]]}) = \{\lambda_{j_1} + \dots + \lambda_{j_k} : \lambda_{j_1}, \dots, \lambda_{j_k} \in \lambda(A_1)\}$.*

Proof. The eigenvalue conclusion follows directly from the tensor product structure (3.10) given in Lemma 3.4 (cf. [62]). \square

Within the framework of Lemma 3.4, the operator D_1 is defined on the tensor product space V^k , which differs from the polynomial space $\mathbb{P}^k[\mathbf{x}]$. The two spaces are not isomorphic - for instance, both tensors $x_1 \otimes x_2, x_2 \otimes x_1 \in V^2$ serve as representations of the same polynomial $x_1 x_2 \in \mathbb{P}^2[\mathbf{x}]$,

whereas their associated multi-indices belong to the same equivalence class defined in Definition 2.1. In what follows, we investigate the relationship between the operator D_1 acting on V^k and the quotient space $\mathbb{P}^k[\mathbf{x}]/\mathbb{P}^{k-1}[\mathbf{x}]$.

Lemma 3.6. *There exists a basis of V^k under which the matrix representation of D_1 is a block upper triangular matrix with the specific form*

$$\begin{bmatrix} A_1^{[[k]]} & * \\ & * \end{bmatrix}. \quad (3.12)$$

Proof. For any multi-index $\alpha \in \mathcal{I}_{d+1}^{[[k]]}$, positive integers $j \in \{1, \dots, k\}$ and $l \in \{1, \dots, d+1\}$, we define $\iota(\alpha; j, l) := (\alpha_1, \dots, \alpha_{j-1}, l, \alpha_{j+1}, \dots, \alpha_k) \in \mathcal{I}_{d+1}^{[[k]]}$ as the multi-index obtained by replacing the j -th component of α with l . Let $\bar{\iota}(\alpha; j, l)$ denote the representative of the equivalence class containing $\iota(\alpha; j, l)$, with its i -th component written as $\bar{\iota}(\alpha; j, l)_i$. When the multi-index α is chosen as a representative element $\bar{\alpha} \in \tilde{\mathcal{I}}_{d+1}^{[[k]]}$, the right-hand side of (3.6) can be expressed more compactly using polynomials generated by the representative multi-indices

$$D_1(\mathbf{x}^{\bar{\alpha}}) = \sum_{j=1}^k \sum_{l=1}^{d+1} (A_1)_{\bar{\alpha}_j l} x_{\bar{\iota}(\bar{\alpha}; j, l)_1} \cdots x_{\bar{\iota}(\bar{\alpha}; j, l)_k} = \sum_{j=1}^k \sum_{l=1}^{d+1} (A_1)_{\bar{\alpha}_j l} x^{\bar{\iota}(\bar{\alpha}; j, l)}. \quad (3.13)$$

Under the basis $P_{\mathbf{x}}^{[k,0]} = \{\mathbf{x}^{\bar{\alpha}} : \bar{\alpha} \in \tilde{\mathcal{I}}_{d+1}^{[[k]]}\}$, the matrix representation of the operator D_1 , defined in (3.13) as a linear mapping on $\mathbb{P}^k[\mathbf{x}]/\mathbb{P}^{k-1}[\mathbf{x}]$, coincides precisely with $A_1^{[[k]]}$. Noting the natural isomorphism between $\mathbb{P}^k[\mathbf{x}]/\mathbb{P}^{k-1}[\mathbf{x}]$ and the subspace $\bar{V}^k := \text{span}\{x_{\bar{\alpha}_1} \otimes \cdots \otimes x_{\bar{\alpha}_k} : \bar{\alpha} \in \tilde{\mathcal{I}}_{d+1}^{[[k]]}\}$ of V^k , we now investigate the relationship between the two representations of D_1 given by (3.13) and Lemma 3.4. For any tensor $\eta \in V^k$, we assume its linear representation

$$\eta = \sum_{\alpha \in \mathcal{I}_{d+1}^{[[k]]}} c_{\alpha} x_{\alpha_1} \otimes \cdots \otimes x_{\alpha_k}, \quad c_{\alpha} \in \mathbb{C}.$$

We define a linear mapping $\Phi : V^k \rightarrow V^k$ by

$$\Phi(\eta) = \sum_{\bar{\alpha} \in \tilde{\mathcal{I}}_{d+1}^{[[k]]}} \sum_{\beta \in [\bar{\alpha}]} c_{\beta} x_{\bar{\alpha}_1} \otimes \cdots \otimes x_{\bar{\alpha}_k} + \sum_{\bar{\alpha} \in \tilde{\mathcal{I}}_{d+1}^{[[k]]}} \sum_{\beta \in [\bar{\alpha}] \setminus \{\bar{\alpha}\}} c_{\beta} x_{\beta_1} \otimes \cdots \otimes x_{\beta_k}. \quad (3.14)$$

The inverse map of Φ is explicitly given by

$$\Phi^{-1}(\eta) = \sum_{\bar{\alpha} \in \tilde{\mathcal{I}}_{d+1}^{[[k]]}} \left(c_{\bar{\alpha}} - \sum_{\beta \in [\bar{\alpha}] \setminus \{\bar{\alpha}\}} c_{\beta} \right) x_{\bar{\alpha}_1} \otimes \cdots \otimes x_{\bar{\alpha}_k} + \sum_{\bar{\alpha} \in \tilde{\mathcal{I}}_{d+1}^{[[k]]}} \sum_{\beta \in [\bar{\alpha}] \setminus \{\bar{\alpha}\}} c_{\beta} x_{\beta_1} \otimes \cdots \otimes x_{\beta_k}. \quad (3.15)$$

Consequently, the set $\{\Phi(x_{\alpha_1} \otimes \cdots \otimes x_{\alpha_k}) : \alpha \in \mathcal{I}_{d+1}^{[[k]]}\}$ forms a basis for V^k . For the tensor $x_{\bar{\alpha}_1} \otimes \cdots \otimes x_{\bar{\alpha}_k}$ generated by representative multi-index $\bar{\alpha} \in \tilde{\mathcal{I}}_{d+1}^{[[k]]}$, (3.14) implies the invariance property $\Phi(x_{\bar{\alpha}_1} \otimes \cdots \otimes x_{\bar{\alpha}_k}) = x_{\bar{\alpha}_1} \otimes \cdots \otimes x_{\bar{\alpha}_k}$. This property demonstrates that the subspace \bar{V}^k remains invariant under the action of Φ (or equivalently, of Φ^{-1}). For each representative element $\bar{\alpha} \in \tilde{\mathcal{I}}_{d+1}^{[[k]]}$, we apply (3.11) and (3.15) to compute

$$\begin{aligned} \Phi D_1 \Phi^{-1} (x_{\bar{\alpha}_1} \otimes \cdots \otimes x_{\bar{\alpha}_k}) &= \sum_{j=1}^k \Phi (x_{\bar{\alpha}_1} \otimes \cdots \otimes D_1(x_{\bar{\alpha}_j}) \otimes \cdots \otimes x_{\bar{\alpha}_k}) \\ &= \sum_{j=1}^k \sum_{l=1}^{d+1} (A_1)_{\bar{\alpha}_j l} \Phi(x_{\bar{\alpha}_1} \otimes \cdots \otimes x_l \otimes \cdots \otimes x_{\bar{\alpha}_k}). \end{aligned}$$

From the definition (2.3) of $\tilde{\mathcal{I}}_{d+1}^{[[k]]}$, we observe that $(\bar{\alpha}_1, \dots, \bar{\alpha}_{j-1}, l, \bar{\alpha}_{j+1}, \dots, \bar{\alpha}_k) \in \tilde{\mathcal{I}}_{d+1}^{[[k]]}$ if and only if $\bar{\alpha}_{j-1} \leq l \leq \bar{\alpha}_{j+1}$. This condition, combined with (3.14), yields

$$\begin{aligned} &\Phi D_1 \Phi^{-1} (x_{\bar{\alpha}_1} \otimes \cdots \otimes x_{\bar{\alpha}_k}) \\ &= \sum_{j=1}^k \left(\sum_{l=1}^{d+1} (A_1)_{\bar{\alpha}_j l} x_{\bar{\ell}(\bar{\alpha}; j, l)_1} \otimes \cdots \otimes x_{\bar{\ell}(\bar{\alpha}; j, l)_k} + \sum_{\substack{l < \bar{\alpha}_{j-1} \\ l > \bar{\alpha}_{j+1}}} (A_1)_{\bar{\alpha}_j l} x_{\bar{\alpha}_1} \otimes \cdots \otimes x_l \otimes \cdots \otimes x_{\bar{\alpha}_k} \right). \quad (3.16) \end{aligned}$$

The first term in (3.16) lies in the subspace \bar{V}^k and matches exactly the form of (3.13), corresponding to a certain row of $A_1^{[[k]]}$. The second term belongs to the complementary space $(\bar{V}^k)^\perp$. Therefore, under the basis $\{\Phi(x_{\alpha_1} \otimes \cdots \otimes x_{\alpha_k}) : \alpha \in \mathcal{I}_{d+1}^{[[k]]}\}$, the action of D_1 on $\{\Phi(x_{\bar{\alpha}_1} \otimes \cdots \otimes x_{\bar{\alpha}_k}) : \bar{\alpha} \in \tilde{\mathcal{I}}_{d+1}^{[[k]]}\}$ coincides with the first row of the block matrix (3.12).

For any $\beta \in [\bar{\alpha}] \setminus \{\bar{\alpha}\}$, applying (3.11), (3.14) and (3.15) gives

$$\begin{aligned}
& \Phi D_1 \Phi^{-1} (x_{\beta_1} \otimes \cdots \otimes x_{\beta_k}) \\
&= \Phi D_1 (-x_{\bar{\alpha}_1} \otimes \cdots \otimes x_{\bar{\alpha}_k} + x_{\beta_1} \otimes \cdots \otimes x_{\beta_k}) \\
&= \sum_{j=1}^k \sum_{l=1}^{d+1} \left(-(A_1)_{\bar{\alpha}_j l} \Phi(x_{\bar{\alpha}_1} \otimes \cdots \otimes x_l \otimes \cdots \otimes x_{\bar{\alpha}_k}) + (A_1)_{\beta_j l} \Phi(x_{\beta_1} \otimes \cdots \otimes x_l \otimes \cdots \otimes x_{\beta_k}) \right) \\
&= - \sum_{j=1}^k \left(\sum_{l=1}^{d+1} (A_1)_{\bar{\alpha}_j l} x_{\bar{\alpha};j,l}_1 \otimes \cdots \otimes x_{\bar{\alpha};j,l}_k + \sum_{\substack{l < \bar{\alpha}_{j-1} \\ l > \bar{\alpha}_{j+1}}} (A_1)_{\bar{\alpha}_j l} x_{\bar{\alpha}_1} \otimes \cdots \otimes x_l \otimes \cdots \otimes x_{\bar{\alpha}_k} \right) \\
&\quad + \sum_{j=1}^k \left(\sum_{l=1}^{d+1} (A_1)_{\beta_j l} x_{\beta;j,l}_1 \otimes \cdots \otimes x_{\beta;j,l}_k + \sum_{\iota(\beta;j,l) \notin \bar{\mathcal{I}}_{d+1}^{[[k]]}} (A_1)_{\beta_j l} x_{\beta_1} \otimes \cdots \otimes x_l \otimes \cdots \otimes x_{\beta_k} \right). \tag{3.17}
\end{aligned}$$

Since β is equivalent to $\bar{\alpha}$ under the equivalence relation \sim , we derive

$$\sum_{j=1}^k \sum_{l=1}^{d+1} (A_1)_{\bar{\alpha}_j l} x_{\bar{\alpha};j,l}_1 \otimes \cdots \otimes x_{\bar{\alpha};j,l}_k = \sum_{j=1}^k \sum_{l=1}^{d+1} (A_1)_{\beta_j l} x_{\beta;j,l}_1 \otimes \cdots \otimes x_{\beta;j,l}_k.$$

The remaining terms in (3.17) are contained in $(\bar{V}^k)^\perp$, yielding $\Phi D_1 \Phi^{-1} ((\bar{V}^k)^\perp) = (\bar{V}^k)^\perp$. This invariance property corresponds to the second row of (3.12). Combining the results from the two cases, we conclude that the operator D_1 admits a block upper triangular matrix representation (3.12) relative to the basis $\{\Phi(x_{\alpha_1} \otimes \cdots \otimes x_{\alpha_k}) : \alpha \in \mathcal{I}_{d+1}^{[[k]]}\}$, thus completing the proof. \square

We immediately conclude that the matrix representation $\mathcal{A}^{[[k]]}$ of the operator D_1 on V^k established in Lemma 3.5 satisfies the diagonalizability and spectral properties stated in Lemma 3.1. Lemma 3.6 establishes an alternative block upper triangular matrix representation (3.12) with $A_1^{[[k]]}$ as its upper-left subblock. The similarity of the two matrix representations ensures that $A_1^{[[k]]}$ satisfies the desired properties. Finally, noting that Lemma 3.3 guarantees the similarity between $A_1^{[k]}(\mathbf{0})$ and $A_1^{[k]}(\hat{\mathbf{x}})$, we complete the proof of Lemma 3.1 by the block structure (3.8). From Lemma 3.1, we directly yield the boundness of the following matrix exponential, which plays a vital role in the convergence analysis.

Lemma 3.7. *Let $\hat{\mathbf{x}}$ be a reference point in a bounded domain independent of ε . The matrix $A_1^{[k]}(\hat{\mathbf{x}})$ is generated in the local linear extension system (2.10). Then*

$$\left\| e^{\frac{1}{\varepsilon} A_1^{[k]}(\hat{\mathbf{x}}) t} \right\| \leq C$$

holds uniformly for any ε, t and $\hat{\mathbf{x}}$.

3.2. Invariant subspaces and block lower triangular diagonalization

This subsection establishes the algebraic properties of diagonalization via a block lower triangular transformation for matrix $A_1^{[k]}(\hat{\mathbf{x}})$. This property is the foundation for implementing adiabatic transformations in the proof of Theorem 4.3. For multi-indices $\beta \in \mathcal{I}_{d+1}^{[[j']]} \cup \mathcal{I}_{d+1}^{[[j]]}$, we define their concatenation as $\beta \oplus \gamma := (\beta_1, \dots, \beta_{j'}, \gamma_1, \dots, \gamma_j) \in \mathcal{I}_{d+1}^{[[j'+j]]}$. We consider multi-indices of the form $\alpha = \beta \oplus \{d+1\}^{\oplus j} \in \mathcal{I}_{d+1}^{[k]}$ such that $\beta \in \mathcal{I}_d^{[[j']]} \cup \mathcal{I}_d^{[[j]]}$ and $0 \leq j' + j \leq k$. Substituting the form of A_1 into (3.6) yields the action of D_1

$$D_1((\mathbf{x} - \hat{\mathbf{x}})^\alpha) = \sum_{l=1}^{j'} \sum_{m=1}^d A_{\beta_l m} (\mathbf{u} - \hat{\mathbf{u}})^{\chi(\beta; l)} (u_m - \hat{u}_m) (t - \hat{t})^j + \sum_{l=1}^{j'} \sum_{m=1}^d A_{\beta_l m} \hat{u}_m (\mathbf{u} - \hat{\mathbf{u}})^{\chi(\beta; l)} (t - \hat{t})^j. \quad (3.18)$$

The lemma for D_1 -invariant subspaces follows directly from (3.18).

Lemma 3.8. Define the subspace $V_{j',j} := \text{span}\{(\mathbf{x} - \hat{\mathbf{x}})^\alpha : \alpha = \beta \oplus \{d+1\}^{\oplus j}, \beta \in \mathcal{I}_d^{[[j']]} \cup \mathcal{I}_d^{[[j]]}\}$.

(i) For any integer $m = 0, \dots, k-j$, the direct sum $\bigoplus_{j'=0}^m V_{j',j}$ constitutes a D_1 -invariant subspace.

(ii) If we take vector $\hat{\mathbf{x}} = \mathbf{0}_{(d+1) \times 1}$, then all corresponding subspaces $V_{j',j} (0 \leq j' + j \leq k)$ are D_1 -invariant.

Among the invariant subspaces characterized in (i) of Lemma 3.8, we focus on the subspace $W_k = \bigoplus_{j'=0}^1 \bigoplus_{j=0}^{k-j'} V_{j',j}$, spanned via the basis $P_{\mathbf{u}}^{[k, \hat{\mathbf{x}}]} := \bigcup_{j'=0}^1 \bigcup_{j=0}^{k-j'} \{(\mathbf{u} - \hat{\mathbf{u}})^{j'} (t - \hat{t})^j\}$. By introducing an appropriate ordering on $P_{\mathbf{u}}^{[k, \hat{\mathbf{x}}]}$, we form an $(k(d+1) + 1)$ -dimensional vector as

$$\mathbf{u}^{[k, \hat{\mathbf{x}}]} := \left[1, (\mathbf{u} - \hat{\mathbf{u}})^\top, t - \hat{t}, (\mathbf{u} - \hat{\mathbf{u}})^\top (t - \hat{t}), \dots, (t - \hat{t})^{k-1}, (\mathbf{u} - \hat{\mathbf{u}})^\top (t - \hat{t})^{k-1}, (t - \hat{t})^k \right]^\top. \quad (3.19)$$

Lemma 3.9. Let the basis elements of $P_{\mathbf{u}}^{[k, \hat{\mathbf{x}}]}$ be ordered according to (3.19). Then the matrix representation $\mathcal{A}_1^{[k]}(\hat{\mathbf{x}})$ of the restricted operator $D_1|_{W_k}$ in this basis has the block structure

$$\mathcal{A}_1^{[k]}(\hat{\mathbf{x}}) = \text{diag}\{I_k \otimes \mathcal{A}_1(\hat{\mathbf{x}}), 0\} \text{ with } \mathcal{A}_1(\hat{\mathbf{x}}) = \begin{bmatrix} 0 & \mathbf{0}_{1 \times d} \\ A\hat{\mathbf{u}} & A \end{bmatrix}. \quad (3.20)$$

Moreover, if Q diagonalizes A such that $Q^{-1}AQ = \Lambda$, then

$$Q_{\mathcal{A}}^{[k]}(\hat{\mathbf{x}}) = \text{diag}\{I_k \otimes Q_{\mathcal{A}}(\hat{\mathbf{x}}), 1\} \text{ with } Q_{\mathcal{A}}(\hat{\mathbf{x}}) = \begin{bmatrix} 1 & \\ -\hat{\mathbf{u}} & Q \end{bmatrix} \quad (3.21)$$

yields the diagonalization of $\mathcal{A}_1^{[k]}(\hat{\mathbf{x}})$ to a canonical form $\text{diag}\{I_k \otimes \text{diag}\{0, \Lambda\}, 0\}$.

Proof. Consider multi-indices of the form $\alpha = l \oplus \{d+1\}^{\oplus j}$ ($l \in \mathcal{I}_d^{[[1]]}$, $j = 0, \dots, k-1$), corresponding to basis elements $(\mathbf{x} - \hat{\mathbf{x}})^\alpha = (u_l - \hat{u}_l)(t - \hat{t})^j \in V_{1,j}$. Then, (3.18) simplifies to

$$D_1((\mathbf{x} - \hat{\mathbf{x}})^\alpha) = \sum_{m=1}^d A_{lm}(u_m - \hat{u}_m)(t - \hat{t})^j + \sum_{m=1}^d A_{lm}\hat{u}_m(t - \hat{t})^j.$$

When $\alpha = \{d+1\}^{\oplus j}$, we obtain the null action $D_1((\mathbf{x} - \hat{\mathbf{x}})^\alpha) = 0$. These computations collectively yield the compact operator representation

$$\begin{aligned} D_1 \left(\begin{bmatrix} (t - \hat{t})^j \\ (\mathbf{u} - \hat{\mathbf{u}})(t - \hat{t})^j \end{bmatrix} \right) &= \mathcal{A}_1(\hat{\mathbf{x}}) \begin{bmatrix} (t - \hat{t})^j \\ (\mathbf{u} - \hat{\mathbf{u}})(t - \hat{t})^j \end{bmatrix}, \quad j = 0, \dots, k-1, \\ D_1((t - \hat{t})^k) &= 0, \end{aligned}$$

where $\mathcal{A}_1(\hat{\mathbf{x}})$ is defined in (3.20). Consequently, under the ordered basis $P_{\mathbf{u}}^{[k, \hat{\mathbf{x}}]}$ specified in (3.19), the matrix representation decomposes as (3.20). The diagonalization property follows from a direct computation and the tensor product formulation. \square

We define the set of j -th degree polynomials $P_{\mathbf{v}}^{[[j, \hat{\mathbf{x}}]]} = P_{\mathbf{x}}^{[[j, \hat{\mathbf{x}}]]} \setminus P_{\mathbf{u}}^{[k, \hat{\mathbf{x}}]} (j = 0, \dots, k)$ via the relative difference of the polynomial sets. It is readily verified that $P_{\mathbf{v}}^{[[0, \hat{\mathbf{x}}]]} = P_{\mathbf{v}}^{[[1, \hat{\mathbf{x}}]]} = \emptyset$. For $j = 2, \dots, k$, the polynomials in $P_{\mathbf{v}}^{[[j, \hat{\mathbf{x}}]]}$ are arranged in an arbitrary order to form the vector $\mathbf{v}^{[[j, \hat{\mathbf{x}}]]}$. Then we define the local linear extension variable under a new ordering as

$$\mathbf{x}^{[k, \hat{\mathbf{x}}]} = \begin{bmatrix} (\mathbf{u}^{[k, \hat{\mathbf{x}}]})^\top & (\mathbf{v}^{[k, \hat{\mathbf{x}}]})^\top \end{bmatrix}^\top, \text{ with } \mathbf{v}^{[k, \hat{\mathbf{x}}]} = \begin{bmatrix} (\mathbf{v}^{[[2, \hat{\mathbf{x}}]]})^\top & \cdots & (\mathbf{v}^{[[k, \hat{\mathbf{x}}]]})^\top \end{bmatrix}^\top. \quad (3.22)$$

While this ordering differs from (2.6) used for numerical constructions, their essential equivalence is claimed in Remark 2.3, allowing our employment of the same notation $\mathbf{x}^{[k, \hat{\mathbf{x}}]}$.

Lemma 3.10. *Suppose the ordering scheme for $\mathbf{x}^{[k, \hat{\mathbf{x}}]}$ is defined by (3.19) and (3.22). Then*

- (i) $A_1^{[k]}(\hat{\mathbf{x}})$ is a block lower triangular matrix with $\mathcal{A}_1^{[k]}(\hat{\mathbf{x}})$ as its upper-left block.
- (ii) $A_1^{[k]}(\hat{\mathbf{x}})$ can be diagonalized by a structurally identical block lower triangular matrix $Q^{[k]}(\hat{\mathbf{x}})$ with $Q_{\mathcal{A}}^{[k]}(\hat{\mathbf{x}})$ as the upper-left block.

Proof. (i) follows from the analysis of matrix representations of D_1 -invariant subspaces in Lemma 3.9, combined with the variable ordering (3.22). For (ii), the conclusion (ii) of Lemma 3.8 implies

that when $\hat{\mathbf{x}} = \mathbf{0}_{(d+1) \times 1}$, the subspaces $\text{span}\{P_{\mathbf{v}}^{[[j, \mathbf{0}]]}\} (j = 2, \dots, k)$ are also D_1 -invariant. Consequently, D_1 admits a block diagonal matrix representation under the basis $P_{\mathbf{u}}^{[k, \hat{\mathbf{x}}]} \cup P_{\mathbf{v}}^{[k, \mathbf{0}]}$, where $P_{\mathbf{v}}^{[k, \mathbf{0}]} = \bigcup_{j=2}^k P_{\mathbf{v}}^{[[j, \mathbf{0}]]}$. This representation, containing $\mathcal{A}_1^{[k]}(\hat{\mathbf{x}})$ as its upper-left subblock, can be clearly diagonalized by a block diagonal matrix having $Q_{\mathcal{A}}^{[k]}(\hat{\mathbf{x}})$ as its upper-left subblock. It remains to analyze the transition matrix from the basis $P_{\mathbf{u}}^{[k, \hat{\mathbf{x}}]} \cup P_{\mathbf{v}}^{[k, \mathbf{0}]}$ to $P_{\mathbf{x}}^{[k, \hat{\mathbf{x}}]}$. Since the polynomials in $\mathbf{v}^{[k, \hat{\mathbf{x}}]}$ are arranged in ascending order by degree according to (3.22), the same analytical approach as in Lemma 3.3 confirms that this transition matrix is lower triangular with all diagonal entries equal to 1. This result gives the existence of the matrix $Q^{[k]}(\hat{\mathbf{x}})$ and concludes the proof. \square

From Lemma 3.9 and 3.10, the following result is obtained through direct matrix computation.

Lemma 3.11. *Under the ordering (3.19) and (3.22), the equality*

$$\Pi_{j(d+1)+1}^{(j+1)(d+1)} \left(Q^{[k]}(\hat{\mathbf{x}}) \right)^{-1} = (Q_{\mathcal{A}}(\hat{\mathbf{x}}))^{-1} \Pi_{j(d+1)+1}^{(j+1)(d+1)}, \quad j = 0, \dots, k-1$$

holds. Specifically, we have

$$\begin{aligned} \Pi_{j(d+1)+1}^{j(d+1)+1} \left(Q^{[k]}(\hat{\mathbf{x}}) \right)^{-1} \mathbf{x}^{[k]} &= (t - \hat{t})^j, \quad j = 0, \dots, k, \\ \Pi_{j(d+1)+2}^{(j+1)(d+1)} \left(Q^{[k]}(\hat{\mathbf{x}}) \right)^{-1} \mathbf{x}^{[k]} &= (t - \hat{t})^j Q^{-1} \mathbf{u}, \quad j = 0, \dots, k-1. \end{aligned}$$

4. Convergence analysis

For notational simplicity, we denote $\mathbf{x}(t_n)$ by \mathbf{x}_n for $n = 0, \dots, N$. We consider the local linear extension variable at solution points \mathbf{x}_n , along with the associated extension system over the interval $[t_n, t_{n+1}]$

$$\begin{aligned} \frac{d\mathbf{x}^{[k, \mathbf{x}_n]}}{dt} &= \frac{1}{\varepsilon} A_1^{[k]}(\mathbf{x}_n) \mathbf{x}^{[k, \mathbf{x}_n]} + A_0^{[k]}(\mathbf{x}_n) \mathbf{x}^{[k, \mathbf{x}_n]} + \mathbf{R}^{[k]}(\mathbf{x}^{[k, \mathbf{x}_n]}), \quad t_n \leq t \leq t_{n+1}, \\ \mathbf{x}^{[k, \mathbf{x}_n]}(t_n) &= e_1, \end{aligned} \tag{4.1}$$

where we introduce the shorthand notation $\mathbf{R}^{[k]}(\mathbf{x}^{[k, \mathbf{x}_n]}) := \mathbf{R}^{[k]}(\mathbf{x}^{[k, \mathbf{x}_n]}; \mathbf{x}_n)$. Taking $\hat{\mathbf{x}} = \mathbf{x}_n$ in Definition 2.2, we have $\Pi_2^{d+2} \mathbf{x}^{[k, \mathbf{x}_n]}(t) = \mathbf{x}(t) - \mathbf{x}_n$, the recovery of the exact solution for (2.1) from solving exactly the local linear extension system (4.1). In particular, we have $\mathbf{x}_{n+1} = \Pi_2^{d+2} \mathbf{x}^{[k, \mathbf{x}_n]}(t_{n+1}) + \mathbf{x}_n$ for $n = 0, \dots, N-1$. The truncated system of (4.1) is again linear, given by

$$\begin{aligned} \frac{d\tilde{\mathbf{x}}^{[k, \mathbf{x}_n]}}{dt} &= \frac{1}{\varepsilon} A_1^{[k]}(\mathbf{x}_n) \tilde{\mathbf{x}}^{[k, \mathbf{x}_n]} + A_0^{[k]}(\mathbf{x}_n) \tilde{\mathbf{x}}^{[k, \mathbf{x}_n]}, \quad t_n \leq t \leq t_{n+1}, \\ \tilde{\mathbf{x}}^{[k, \mathbf{x}_n]}(t_n) &= e_1. \end{aligned} \tag{4.2}$$

We use an analogous notation for the projected solution $\tilde{\mathbf{x}}_{n+1} := \Pi_2^{d+2} \tilde{\mathbf{x}}^{[k, \mathbf{x}_n]}(t_{n+1}) + \mathbf{x}_n$. With the help of the intermediate system (4.2), the error analysis focuses on the difference between the exact solution \mathbf{x}_{n+1} , obtained by the extension system (4.1), and the approximation solution \mathbf{X}_{n+1} , projected from the truncated system (2.12). Throughout the analysis, we always assume the derivatives of \mathbf{F} are Lipschitz continuous up to order k in both \mathbf{u} and t .

4.1. Convergence results when $h < \varepsilon$

This subsection demonstrates the high-order uniform accuracy conclusions under small time-step conditions.

Lemma 4.1. *Let $\mathbf{u}(t)$ be solution of (1.1) that stay in a bounded domain independent of ε for $t \in [0, T]$. The ordering scheme for the extension variables is defined by (2.6). Let $\rho = \max |\lambda(A)|$ denote the spectral radius of A . Then there exists a positive constant $h_0 < \frac{\pi\varepsilon}{2\rho}$ such that for all $h < h_0$,*

$$\left\| \Pi_2^{d+2} \mathbf{x}^{[k, \mathbf{x}_n]}(t_{n+1}) \right\| \leq Ch,$$

where the constant C is independent of h and ε .

Proof. Applying variation-of-constants formula to systems (4.1), we obtain

$$\mathbf{x}^{[k, \mathbf{x}_n]}(t) = e^{\frac{1}{\varepsilon} A_1^{[k]}(\mathbf{x}_n)(t-t_n)} e_1 + \int_{t_n}^t e^{\frac{1}{\varepsilon} A_1^{[k]}(\mathbf{x}_n)(t-s)} A_0^{[k]}(\mathbf{x}_n) \mathbf{x}^{[k, \mathbf{x}_n]}(s) ds + \int_{t_n}^t e^{\frac{1}{\varepsilon} A_1^{[k]}(\mathbf{x}_n)(t-s)} \mathbf{R}^{[k]}(\mathbf{x}^{[k, \mathbf{x}_n]}(s)) ds. \quad (4.3)$$

Lemma 3.7 ensures the ε -independent upper bound for the matrix exponential. Since the non-zero entries of $A_0^{[k]}(\cdot)$ are products of partial derivatives of \mathbf{F} and polynomial terms, $A_0^{[k]}(\cdot)$ remains bounded. Taking the norm on both sides of (4.3) and applying the integral form of Gronwall's inequality, we derive the boundedness of the high-dimensional solution $\mathbf{x}^{[k, \mathbf{x}_n]}(t)$ on $[t_n, t_{n+1}]$. Consequently, the two integrals in (4.3) evaluated at $t = t_{n+1}$ are bounded by $O(h)$. To complete the proof of the lemma, it remains to establish the estimate

$$\left\| \Pi_2^{d+2} e^{\frac{1}{\varepsilon} A_1^{[k]}(\mathbf{x}_n)h} e_1 \right\| \leq Ch. \quad (4.4)$$

By Lemma 3.3, the matrix $A_1^{[k]}(\mathbf{x}_n)$ is similar to $A_1^{[k]}(\mathbf{0})$, with the similarity transformation given explicitly in (3.7). Using the diagonal structure of $A_1^{[k]}(\mathbf{0})$ from (3.8), we derive

$$\Pi_2^{d+2} e^{\frac{1}{\varepsilon} A_1^{[k]}(\mathbf{x}_n)h} e_1 = \Pi_2^{d+2} S^{[k]}(\mathbf{x}_n) e^{\frac{1}{\varepsilon} A_1^{[k]}(\mathbf{0})h} \left(S^{[k]}(\mathbf{x}_n) \right)^{-1} e_1 = \left(e^{\frac{1}{\varepsilon} A_1 h} - I_{d+1} \right) \mathbf{x}_n, \quad (4.5)$$

through direct matrix multiplication. Denote the canonical form of A_1 by the complex diagonal matrix $\Lambda_1 = \text{diag}\{\text{i}\lambda_1, \dots, \text{i}\lambda_{d+1}\}$ with the similar transformation Q_1 . We have

$$e^{\frac{1}{\varepsilon}A_1h} - I_{d+1} = Q_1 \text{diag}\{e^{\frac{1}{\varepsilon}\lambda_1h} - 1, \dots, e^{\frac{1}{\varepsilon}\lambda_{d+1}h} - 1\}Q_1^{-1}.$$

The condition $h < h_0$ implies $\frac{1}{\varepsilon}|\lambda_j|h < \frac{\pi}{2}$ for $j = 1, \dots, d+1$. Then we obtain

$$\left|e^{\frac{1}{\varepsilon}\lambda_jh} - 1\right| \leq \left|\cos \frac{1}{\varepsilon}\lambda_jh - 1\right| + \left|\sin \frac{1}{\varepsilon}\lambda_jh\right| \leq 1 - \cos \frac{\pi h}{2h_0} + \sin \frac{\pi h}{2h_0} \leq Ch, \quad h < h_0.$$

Consequently, the uniform bound $\left\|e^{\frac{1}{\varepsilon}A_1h} - I_{d+1}\right\| \leq Ch$ holds. The estimate (4.4) follows directly by substituting this bound into (4.5). \square

Theorem 4.2. *Let $\mathbf{u}(t)$ be solution of (1.1) and $\mathbf{U}_n (n = 0, \dots, T/h)$ be the numerical solution computed by (2.13)-(2.15). Under the condition in Lemma 4.1, we have*

$$\|\mathbf{U}_n - \mathbf{u}(t_n)\| \leq Ch^{k+1}, \quad n = 0, \dots, T/h,$$

for $h < h_0$, where the constant C depends on A, T, k, u_0 and the function \mathbf{F} but is independent of h and ε .

Proof. Local estimate. We apply the variation-of-constants formula to (4.2) and yield

$$\tilde{\mathbf{x}}^{[k, \mathbf{x}_n]}(t) = e^{\frac{1}{\varepsilon}A_1^{[k]}(\mathbf{x}_n)(t-t_n)}e_1 + \int_{t_n}^t e^{\frac{1}{\varepsilon}A_1^{[k]}(\mathbf{x}_n)(t-s)}A_0^{[k]}(\mathbf{x}_n)\tilde{\mathbf{x}}^{[k, \mathbf{x}_n]}(s)ds. \quad (4.6)$$

Subtracting (4.6) from (4.3) gives

$$\begin{aligned} \mathcal{R}_1^{[k]}(t) &:= \mathbf{x}^{[k, \mathbf{x}_n]}(t) - \tilde{\mathbf{x}}^{[k, \mathbf{x}_n]}(t) \\ &= \int_{t_n}^t e^{\frac{1}{\varepsilon}A_1^{[k]}(\mathbf{x}_n)(t-s)}A_0^{[k]}(\mathbf{x}_n)\left(\mathbf{x}^{[k, \mathbf{x}_n]}(s) - \tilde{\mathbf{x}}^{[k, \mathbf{x}_n]}(s)\right)ds + \int_{t_n}^t e^{\frac{1}{\varepsilon}A_1^{[k]}(\mathbf{x}_n)(t-s)}\mathbf{R}^{[k]}(\mathbf{x}^{[k, \mathbf{x}_n]}(s))ds. \end{aligned} \quad (4.7)$$

We estimate (4.7) at $t = t_{n+1}$. From Lemma 4.1, we have $\|\mathbf{x}_{n+1} - \mathbf{x}_n\| = \|\Pi_2^{d+2}\mathbf{x}^{[k, \mathbf{x}_n]}(t_{n+1})\| \leq Ch$. Consequently, the j -th order Taylor remainder terms \mathbf{r}^j of \mathbf{F} satisfy $\|\mathbf{r}^j(\mathbf{x}_{n+1}; \mathbf{x}_n)\| \leq Ch^j$ for $j = 2, \dots, k+1$. Noting that each component of $\mathbf{R}^{[k]}$ can be expressed by (2.11) with $\mathbf{x} = \mathbf{x}_{n+1}$ and $\hat{\mathbf{x}} = \mathbf{x}_n$, we derive $\|\mathbf{R}^{[k]}(\mathbf{x}^{[k, \mathbf{x}_n]}(t_{n+1}))\| \leq Ch^{k+1}$. Substituting the approximation of $\|\mathbf{R}^{[k]}\|$ into (4.7) yields

$$\|\mathcal{R}_1^{[k]}(t_{n+1})\| \leq C \int_{t_n}^{t_{n+1}} \|\mathbf{x}^{[k, \mathbf{x}_n]}(s) - \tilde{\mathbf{x}}^{[k, \mathbf{x}_n]}(s)\|ds + Ch^{k+2}.$$

The local error estimate for $h < h_0$ follows through the integral form of Gronwall inequality

$$\|\mathcal{R}_1^{[k]}(t_{n+1})\| = \|\mathbf{x}^{[k, \mathbf{x}_n]}(t_{n+1}) - \tilde{\mathbf{x}}^{[k, \mathbf{x}_n]}(t_{n+1})\| \leq Ch^{k+2}. \quad (4.8)$$

Global estimate. Applying the nonsingular transformations from Lemma 3.3, we introduce the variable substitutions $\mathbf{X}^{[k, \mathbf{0}]} = (S^{[k]}(\mathbf{X}_n))^{-1} \mathbf{X}^{[k, \mathbf{X}_n]}$ and $\tilde{\mathbf{x}}^{[k, \mathbf{0}]} = (S^{[k]}(\mathbf{x}_n))^{-1} \tilde{\mathbf{x}}^{[k, \mathbf{x}_n]}$ into systems (4.2) and (2.12), respectively. This transformation yields the systems

$$\frac{d\tilde{\mathbf{x}}^{[k, \mathbf{0}]}}{dt} = \frac{1}{\varepsilon} A_1^{[k]}(\mathbf{0}) \tilde{\mathbf{x}}^{[k, \mathbf{0}]} + \bar{A}_0^{[k]}(\mathbf{x}_n) \tilde{\mathbf{x}}^{[k, \mathbf{0}]}, \quad \tilde{\mathbf{x}}^{[k, \mathbf{0}]}(t_n) = (S^{[k]}(\mathbf{x}_n))^{-1} e_1,$$

and

$$\frac{d\mathbf{X}^{[k, \mathbf{0}]}}{dt} = \frac{1}{\varepsilon} A_1^{[k]}(\mathbf{0}) \mathbf{X}^{[k, \mathbf{0}]} + \bar{A}_0^{[k]}(\mathbf{X}_n) \mathbf{X}^{[k, \mathbf{0}]}, \quad \mathbf{X}^{[k, \mathbf{0}]}(t_n) = (S^{[k]}(\mathbf{X}_n))^{-1} e_1,$$

where $\bar{A}_0^{[k]}(\hat{\mathbf{x}}) = (S^{[k]}(\hat{\mathbf{x}}))^{-1} A_0^{[k]}(\hat{\mathbf{x}}) S^{[k]}(\hat{\mathbf{x}})$. Using the variation-of-constants formula and subtracting the two expressions, we obtain

$$\tilde{\mathbf{x}}^{[k, \mathbf{0}]}(t) - \mathbf{X}^{[k, \mathbf{0}]}(t) = e^{\frac{1}{\varepsilon} A_1^{[k]}(\mathbf{0})(t-t_n)} \left((S^{[k]}(\mathbf{x}_n))^{-1} - (S^{[k]}(\mathbf{X}_n))^{-1} \right) e_1 + \mathcal{R}_2^{[k]}(t), \quad (4.9)$$

with $\mathcal{R}_2^{[k]}(t)$ defined as

$$\begin{aligned} \mathcal{R}_2^{[k]}(t) &:= \int_{t_n}^t e^{\frac{1}{\varepsilon} A_1^{[k]}(\mathbf{0})(t-s)} \left(\bar{A}_0^{[k]}(\mathbf{x}_n) \tilde{\mathbf{x}}^{[k, \mathbf{0}]}(s) - \bar{A}_0^{[k]}(\mathbf{X}_n) \mathbf{X}^{[k, \mathbf{0}]}(s) \right) ds \\ &= \int_{t_n}^t e^{\frac{1}{\varepsilon} A_1^{[k]}(\mathbf{0})(t-s)} \left(\bar{A}_0^{[k]}(\mathbf{x}_n) - \bar{A}_0^{[k]}(\mathbf{X}_n) \right) \tilde{\mathbf{x}}^{[k, \mathbf{0}]}(s) ds \\ &\quad + \int_{t_n}^t e^{\frac{1}{\varepsilon} A_1^{[k]}(\mathbf{0})(t-s)} \bar{A}_0^{[k]}(\mathbf{X}_n) (\tilde{\mathbf{x}}^{[k, \mathbf{0}]}(s) - \mathbf{X}^{[k, \mathbf{0}]}(s)) ds. \end{aligned} \quad (4.10)$$

By Lemma 3.3, both $S^{[k]}(\cdot)$ and its inverse are Lipschitz continuous. The Lipschitz continuity of $A_0^{[k]}(\cdot)$ stems from its construction via products of polynomials and partial derivatives of \mathbf{F} . These observations imply that $\bar{A}_0^{[k]}(\cdot)$ is also Lipschitz continuous. From (4.9) and (4.10), we then derive the inequality

$$\|\tilde{\mathbf{x}}^{[k, \mathbf{0}]}(t) - \mathbf{X}^{[k, \mathbf{0}]}(t)\| \leq C \|\mathbf{x}_n - \mathbf{X}_n\| + C \int_{t_n}^t \|\tilde{\mathbf{x}}^{[k, \mathbf{0}]}(s) - \mathbf{X}^{[k, \mathbf{0}]}(s)\| ds.$$

Applying the integral form of Gronwall's inequality yields the estimate

$$\|\tilde{\mathbf{x}}^{[k, \mathbf{0}]}(t) - \mathbf{X}^{[k, \mathbf{0}]}(t)\| \leq C e^{Ct} \|\mathbf{x}_n - \mathbf{X}_n\|, \quad t_n \leq t \leq t_{n+1}. \quad (4.11)$$

Exploiting (4.11) to bound the second term in (4.10), we obtain the estimate for $\mathcal{R}_2^{[k]}(t_{n+1})$

$$\|\mathcal{R}_2^{[k]}(t_{n+1})\| \leq C \|\mathbf{x}_n - \mathbf{X}_n\|. \quad (4.12)$$

Note that when $\hat{\mathbf{x}} = \mathbf{0}$, Definition 2.2 implies that the projection Π_2^{d+2} applied to the extension variables recovers the original variables. We individually project equations (4.7) and (4.9), then combine the results. Using the matrix structures given in (3.7) and (3.8), we derive the recurrence relation

$$\mathbf{x}_{n+1} - \mathbf{X}_{n+1} = e^{\frac{1}{\varepsilon} A_1 h} (\mathbf{x}_n - \mathbf{X}_n) + \Pi_2^{d+2} \left(\mathcal{R}_1^{[k]}(t_{n+1}) + \mathcal{R}_2^{[k]}(t_{n+1}) \right).$$

Solving this recurrence relation with $\mathbf{x}_0 = \mathbf{X}_0$, we obtain

$$\mathbf{x}_n - \mathbf{X}_n = \sum_{j=1}^n e^{\frac{n-j}{\varepsilon} A_1 h} \Pi_2^{d+2} \left(\mathcal{R}_1^{[k]}(t_j) + \mathcal{R}_2^{[k]}(t_j) \right). \quad (4.13)$$

Substituting the bounds for $\mathcal{R}_i^{[k]}(i = 1, 2)$ from (4.8) and (4.12) into (4.13), and invoking Lemma 3.7, we obtain the inequality

$$\|\mathbf{x}_n - \mathbf{X}_n\| \leq \sum_{j=1}^n (C \|\mathbf{x}_{j-1} - \mathbf{X}_{j-1}\| + Ch^{k+2}).$$

Finally, an application of the discrete Gronwall inequality yields the desired error estimate. \square

4.2. Convergence results with bounded oscillatory energy when $h > \varepsilon$

Assuming $\nu \geq 1$ in (1.1), we now establish the improved uniform accuracy results for the local linear exponential integrators applied to (1.1) under large time steps $h > \varepsilon$. This case, characterized by bounded oscillatory energy in physical systems (1.4), is common in practical applications [13, 7].

Theorem 4.3. *Let $\nu \geq 1$ such that $\mathbf{u}(t)$ in (1.1) satisfies the bounded oscillatory energy condition on $t \in [0, T]$, and \mathbf{U}_n be the numerical solution to (1.1) defined in Section 2. The ordering scheme for extension variables is defined by (3.19) and (3.22). Let $\mu = \min |\lambda(A)|$ denote the minimal magnitude of the eigenvalues of A . Then there exist two positive constants $\underline{h}_0 > \frac{2\pi\varepsilon}{\mu}$ and $\overline{h}_0 < (C\varepsilon)^{-1}$, such that for $\underline{h}_0 < h < \overline{h}_0$*

$$\|\mathbf{U}_n - \mathbf{u}(t_n)\| \leq C\varepsilon h^k, \quad n = 0, \dots, T/h,$$

where the constant C depends on A , T , k , u_0 and the function \mathbf{F} but is independent of h and ε .

We remark that Lemma 3.1 only guarantees zero real parts for eigenvalues of $A_1^{[k]}$, without excluding additional zero eigenvalues beyond those introduced by $\mathbf{x}^{[[0, \hat{\mathbf{x}}]]}$ (see Lemma 3.5). This situation arises particularly when system (1.1) represents the first-order reformulation of the second-order equation (1.2), where the conjugate eigenvalue pairs of matrix A inherently result in the

existence of additional zero eigenvalues. The non-oscillatory modes associated with these zero eigenvalues present additional analytical challenges. To overcome this difficulty, we separate the oscillatory and non-oscillatory components as our primary methodology in the proof.

Proof. Adiabatic transformation. We first apply adiabatic transformation

$$\mathbf{w}^{[k, \mathbf{x}_n]} = e^{-\frac{1}{\varepsilon} \Lambda_1^{[k]} t} \left(Q^{[k]}(\mathbf{x}_n) \right)^{-1} \mathbf{x}^{[k, \mathbf{x}_n]},$$

where the diagonal matrix $\Lambda_1^{[k]} = (Q^{[k]}(\mathbf{x}_n))^{-1} A_1^{[k]}(\mathbf{x}_n) Q^{[k]}(\mathbf{x}_n)$ and the block lower triangular matrix $Q^{[k]}(\mathbf{x}_n)$, defined in Lemma 3.10, contains (3.21) as upper-left subblock. Applying analogous adiabatic transformation to $\mathbf{u}(t)$ with $\mathbf{w}(t) = e^{-\frac{1}{\varepsilon} \Lambda t} Q^{-1} \mathbf{u}(t)$, where Q and Λ are as defined in Lemma 3.9, and invoking Lemma 3.11, we obtain

$$\Pi_2^{d+1} \mathbf{w}^{[k, \mathbf{x}_n]}(t) = \mathbf{w}(t). \quad (4.14)$$

This equation demonstrates that the relationship between the adiabatic variables $\mathbf{w}^{[k, \mathbf{x}_n]}(t)$ and $\mathbf{w}(t)$ preserves the original correspondence between $\mathbf{x}^{[k, \mathbf{x}_n]}(t)$ and $\mathbf{x}(t)$. A similar high-dimensional adiabatic variable is introduced via $\tilde{\mathbf{w}}^{[k, \mathbf{x}_n]} = e^{-\frac{1}{\varepsilon} \Lambda_1^{[k]} t} (Q^{[k]}(\mathbf{x}_n))^{-1} \tilde{\mathbf{x}}^{[k, \mathbf{x}_n]}$ to $\tilde{\mathbf{x}}^{[k, \mathbf{x}_n]}$ associated with the truncated system (4.2). By using the adiabatic variables, (4.7) is reformulated into

$$\begin{aligned} \mathbf{w}^{[k, \mathbf{x}_n]}(t) - \tilde{\mathbf{w}}^{[k, \mathbf{x}_n]}(t) &= \int_{t_n}^t e^{-\frac{1}{\varepsilon} \Lambda_1^{[k]} s} \left(Q^{[k]}(\mathbf{x}_n) \right)^{-1} A_0^{[k]}(\mathbf{x}_n) Q^{[k]}(\mathbf{x}_n) e^{\frac{1}{\varepsilon} \Lambda_1^{[k]} s} \left(\mathbf{w}^{[k, \mathbf{x}_n]}(s) - \tilde{\mathbf{w}}^{[k, \mathbf{x}_n]}(s) \right) ds \\ &\quad + \int_{t_n}^t e^{-\frac{1}{\varepsilon} \Lambda_1^{[k]} s} \left(Q^{[k]}(\mathbf{x}_n) \right)^{-1} \mathbf{R}^{[k]} \left(Q^{[k]}(\mathbf{x}_n) e^{\frac{1}{\varepsilon} \Lambda_1^{[k]} s} \mathbf{w}^{[k, \mathbf{x}_n]}(s) \right) ds. \end{aligned} \quad (4.15)$$

In what follows, we perform a row-wise analysis on the second integral in (4.7).

Estimate for the second integral restricted on the first $k(d+1)+1$ rows in (4.7).

By the ordering scheme of $\mathbf{x}^{[k, \mathbf{x}_n]}$ in (3.19), the rows $j(d+1)+1$ ($j = 0, \dots, k$) corresponds to the polynomials depend solely on t , thus contributing no residual to $\mathbf{R}^{[k]}$, which results in zero rows for the second integral in (4.7). The analysis is first conducted for rows 2 through $d+1$ by employing the adiabatic variable formulation (4.15) for analytical convenience. Followed by Lemma 3.11 and the residual term in (2.11), the second integral in (4.15), when restricted to these rows, takes the form

$$\int_{t_n}^t e^{-\frac{1}{\varepsilon} \Lambda s} Q^{-1} \mathbf{r}_n^{k+1} \left(Q e^{\frac{1}{\varepsilon} \Lambda s} \mathbf{w}(s) \right) ds,$$

where \mathbf{r}_n^{k+1} denotes the residual of \mathbf{r}^{k+1} , evaluated at $(\mathbf{u}(t_n), t_n)$. Consider the q -th row ($1 \leq q \leq d$) with integral form

$$\int_{t_n}^{t_{n+1}} e^{-\frac{1}{\varepsilon} \lambda_q s} \beta_q(s) ds, \quad (4.16)$$

where

$$\beta_q(s) = \sum_{p=1}^d (Q^{-1})_{qp} r_{n,p}^{k+1} \left(Q e^{\frac{1}{\varepsilon} \Lambda s} \mathbf{w}(s) \right).$$

Note that the oscillator $e^{-\frac{i}{\varepsilon} \lambda_q s}$ has period $\frac{2\pi\varepsilon}{|\lambda_q|}$. Our theorem's condition $\frac{2\pi\varepsilon}{\mu} \leq h$ guarantees the existence of a unique integer $N_q \geq 1$ for each q satisfying

$$\frac{2\pi\varepsilon}{|\lambda_q|} N_q \leq t_{n+1} - t_n \leq \frac{2\pi\varepsilon}{|\lambda_q|} (N_q + 1). \quad (4.17)$$

Then the integral (4.16) decomposes as

$$\begin{aligned} & \int_{t_n}^{t_{n+1}} e^{-\frac{i}{\varepsilon} \lambda_q s} \beta_q(s) ds \\ &= \left(\sum_{r=1}^{N_q} \left(\int_{t_n + \frac{2\pi\varepsilon}{|\lambda_q|} r - \frac{2\pi\varepsilon}{|\lambda_q|}}^{t_n + \frac{2\pi\varepsilon}{|\lambda_q|} r - \frac{\pi\varepsilon}{|\lambda_q|}} + \int_{t_n + \frac{2\pi\varepsilon}{|\lambda_q|} r - \frac{\pi\varepsilon}{|\lambda_q|}}^{t_n + \frac{2\pi\varepsilon}{|\lambda_q|} r} \right) + \int_{t_n + \frac{2\pi\varepsilon}{|\lambda_q|} N_q}^{t_{n+1}} \right) e^{-\frac{i}{\varepsilon} \lambda_q s} \beta_q(s) ds \\ &= \sum_{r=1}^{N_q} \int_{t_n + \frac{2\pi\varepsilon}{|\lambda_q|} r - \frac{2\pi\varepsilon}{|\lambda_q|}}^{t_n + \frac{2\pi\varepsilon}{|\lambda_q|} r - \frac{\pi\varepsilon}{|\lambda_q|}} e^{-\frac{i}{\varepsilon} \lambda_q s} \left(\beta_q(s) - \beta_q \left(s + \frac{\pi\varepsilon}{|\lambda_q|} \right) \right) ds + \int_{t_n + \frac{2\pi\varepsilon}{|\lambda_q|} N_q}^{t_{n+1}} e^{-\frac{i}{\varepsilon} \lambda_q s} \beta_q(s) ds. \end{aligned} \quad (4.18)$$

Under bounded oscillatory energy and large time step size conditions, (2.11) still yields the bound $\|\mathbf{r}_n^{k+1}\| \leq Ch^{k+1}$. Applying (4.17), we bound the second integral in (4.18) by

$$\left\| \int_{t_n + \frac{2\pi\varepsilon}{|\lambda_q|} N_q}^{t_{n+1}} e^{-\frac{i}{\varepsilon} \lambda_q s} \beta_q(s) ds \right\| \leq \left(t_{n+1} - t_n - \frac{2\pi\varepsilon}{|\lambda_q|} N_q \right) \|\beta_q(s)\| \leq C\varepsilon h^{k+1}. \quad (4.19)$$

From the original system (1.1), the adiabatic variable $\mathbf{w}(t)$ satisfies

$$\frac{d\mathbf{w}}{dt} = e^{-\frac{1}{\varepsilon} \Lambda t} Q^{-1} \mathbf{F} \left(Q e^{\frac{1}{\varepsilon} \Lambda t} \mathbf{w}(s) \right).$$

Then we have

$$\begin{aligned} \beta_q(s) - \beta_q \left(s + \frac{\pi\varepsilon}{|\lambda_q|} \right) &= - \sum_{p=1}^d (Q^{-1})_{qp} \int_0^{\frac{\pi\varepsilon}{|\lambda_q|}} \frac{d}{d\theta} r_{n,p}^{k+1} \left(Q e^{\frac{1}{\varepsilon} \Lambda(s+\theta)} \mathbf{w}(s+\theta) \right) d\theta \\ &= - \sum_{p=1}^d (Q^{-1})_{qp} \int_0^{\frac{\pi\varepsilon}{|\lambda_q|}} \nabla r_{n,p}^{k+1}(\mathbf{u}(s+\theta)) \left(\frac{1}{\varepsilon} Q \Lambda e^{\frac{1}{\varepsilon} \Lambda(s+\theta)} \mathbf{w}(s+\theta) + \mathbf{F}(\mathbf{u}(s+\theta)) \right) d\theta. \end{aligned}$$

Observing the smooth dependence of $\nabla r_{n,p}^{k+1}(\mathbf{u}(s+\theta))$ on \mathbf{u} , the bounded oscillatory energy condition, along with the boundedness of \mathbf{F} , yields

$$\left\| \beta_q(s) - \beta_q \left(s + \frac{\pi\varepsilon}{|\lambda_q|} \right) \right\| \leq C \int_0^{\frac{\pi\varepsilon}{|\lambda_q|}} \|\nabla r_n^{k+1}(\mathbf{u}(s+\theta))\| \left(\frac{1}{\varepsilon} \|\mathbf{w}(s+\theta)\| + \|\mathbf{F}(\mathbf{u}(s+\theta))\| \right) d\theta \leq C\varepsilon h^k. \quad (4.20)$$

Substituting (4.19), (4.20) and (4.17) into (4.18), we obtain for all $q = 1, \dots, d$

$$\begin{aligned} \left\| \int_{t_n}^{t_{n+1}} e^{-\frac{1}{\varepsilon} \lambda_q s} \beta_q(s) ds \right\| &\leq \sum_{r=1}^{N_q} \int_{t_n + \frac{2\pi\varepsilon}{|\lambda_q|} r - \frac{\pi\varepsilon}{|\lambda_q|}}^{t_n + \frac{2\pi\varepsilon}{|\lambda_q|} r - \frac{\pi\varepsilon}{|\lambda_q|}} C \left\| \beta_q(s) - \beta_q \left(s + \frac{\pi\varepsilon}{|\lambda_q|} \right) \right\| ds + \left\| \int_{t_n + \frac{2\pi\varepsilon}{|\lambda_q|} N_q}^{t_{n+1}} e^{-\frac{1}{\varepsilon} \lambda_q s} \beta_q(s) ds \right\| \\ &\leq C N_q \frac{\pi\varepsilon^2 h^k}{|\lambda_q|} + C\varepsilon h^{k+1} \\ &\leq C\varepsilon h^{k+1}. \end{aligned}$$

Consequently, when transformed back to the original variables, the second integral in (4.7), restricted to the rows 2 through $d+1$, satisfies the bound

$$\left\| \Pi_2^{d+1} \int_{t_n}^{t_{n+1}} e^{\frac{1}{\varepsilon} A_1^{[k]}(\mathbf{x}_n)(t-s)} \mathbf{R}^{[k]}(\mathbf{x}^{[k, \mathbf{x}_n]}(s)) ds \right\| \leq C \left\| \int_{t_n}^{t_{n+1}} e^{-\frac{1}{\varepsilon} \Lambda s} Q^{-1} \mathbf{r}_n^{k+1} \left(Q e^{\frac{1}{\varepsilon} \Lambda s} \mathbf{w}(s) \right) ds \right\| \leq C\varepsilon h^{k+1}. \quad (4.21)$$

The same methodology extends naturally to rows $j(d+1)+2$ through $(j+1)(d+1)$ for $j = 1, \dots, k-1$.

According to Lemma 3.11, we obtain $\Pi_{j(d+1)+2}^{(j+1)(d+1)} \mathbf{w}^{[k, \mathbf{x}_n]}(t) = (t-t_n)^j \mathbf{w}(t)$ analogous to (4.14). From (2.11), the remainder terms for these rows reduce to $(t-t_n)^j \mathbf{r}_n^{k-j+1}$, bounded again by $O(h^{k+1})$.

These observations ensure that the error bound established in (4.21) remains valid for all the first $k(d+1)+1$ rows, which correspond to the variables in $P_{\mathbf{u}}^{[k, \mathbf{x}_n]}$.

Local estimate. Turning to the polynomials in $P_{\mathbf{v}}^{[k, \mathbf{x}_n]}$, we observe that for any $(\mathbf{x} - \mathbf{x}_n)^\alpha \in P_{\mathbf{v}}^{[k, \mathbf{x}_n]}$, the multi-index α contains at least two components distinct from $d+1$, as evident from (3.19). Thus, using Lemma 3.1 and the bounded oscillatory energy condition, we have

$$\left\| \Pi_1^{k(d+1)+1} \int_{t_n}^{t_{n+1}} e^{\frac{1}{\varepsilon} A_1^{[k]}(\mathbf{x}_n)(t-s)} A_0^{[k]}(\mathbf{x}_n) (\Pi_{k(d+2)+1}^{D^{[k]}})^\top \left(\mathbf{v}^{[k, \mathbf{x}_n]}(s) - \tilde{\mathbf{v}}^{[k, \mathbf{x}_n]}(s) \right) ds \right\| \leq C\varepsilon^2 h. \quad (4.22)$$

Restricting our analysis to the first $k(d+1)+1$ rows of (4.7) and substituting estimates (4.21) and (4.22) with the projection operator replaced by $\Pi_1^{k(d+1)+1}$, we derive the estimate

$$\begin{aligned} &\| \mathbf{u}^{[k, \mathbf{x}_n]}(t_{n+1}) - \tilde{\mathbf{u}}^{[k, \mathbf{x}_n]}(t_{n+1}) \| \\ &\leq \left\| \Pi_1^{k(d+1)+1} \int_{t_n}^{t_{n+1}} e^{\frac{1}{\varepsilon} A_1^{[k]}(\mathbf{x}_n)(t-s)} A_0^{[k]}(\mathbf{x}_n) (\Pi_1^{k(d+1)+1})^\top \left(\mathbf{u}^{[k, \mathbf{x}_n]}(s) - \tilde{\mathbf{u}}^{[k, \mathbf{x}_n]}(s) \right) ds \right\| + C(\varepsilon^2 h + \varepsilon h^{k+1}) \\ &\leq \int_{t_n}^{t_{n+1}} \left\| e^{\frac{1}{\varepsilon} A_1^{[k]}(\mathbf{x}_n)(t-s)} A_0^{[k]}(\mathbf{x}_n) \right\| \| \mathbf{u}^{[k, \mathbf{x}_n]}(s) - \tilde{\mathbf{u}}^{[k, \mathbf{x}_n]}(s) \| ds + C(\varepsilon^2 h + \varepsilon h^{k+1}). \end{aligned}$$

Through application of the Gronwall's inequality in integral form and further invoking Lemma 3.1, we establish a local estimate for (4.7) over these rows

$$\| \mathbf{u}^{[k, \mathbf{x}_n]}(t_{n+1}) - \tilde{\mathbf{u}}^{[k, \mathbf{x}_n]}(t_{n+1}) \| \leq C(\varepsilon^2 h + \varepsilon h^{k+1}). \quad (4.23)$$

This result immediately implies an error bound $\|\mathbf{x}_{n+1} - \tilde{\mathbf{x}}_{n+1}\| = \|\mathbf{x}^{[[1, \mathbf{x}_n]]}(t_{n+1}) - \tilde{\mathbf{x}}^{[[1, \mathbf{x}_n]]}(t_{n+1})\| \leq C(\varepsilon^2 h + \varepsilon h^{k+1})$ for \mathbf{x} . For the remaining rows, we note that Lemma 3.5 does not preclude the existence of zero eigenvalues in the lower-right subblock for $A_1^{[k]}(\mathbf{x}_n)$. In such cases, the previous time step decomposition approach based on high-frequency periodicity becomes inapplicable. To address this challenge, we exploit the inherent structure of local linear extension variables. For any element $(\mathbf{x} - \mathbf{x}_n)^\alpha \in P_{\mathbf{v}}^{[k, \mathbf{x}_n]}$ with $|\alpha| = j \geq 2$, the product difference formula

$$(\mathbf{x}_{n+1} - \mathbf{x}_n)^\alpha - (\tilde{\mathbf{x}}_{n+1} - \mathbf{x}_n)^\alpha = \sum_{l=1}^j (x_{n+1, \alpha_l} - \tilde{x}_{n+1, \alpha_l}) \prod_{m=1}^{l-1} (\tilde{x}_{n+1, \alpha_m} - x_{n, \alpha_m}) \prod_{m=l+1}^j (x_{n+1, \alpha_m} - x_{n, \alpha_m})$$

holds according to Definition 2.2. Since α contains at least two components distinct from $d+1$, taking norms yields the estimate

$$\|(\mathbf{x}_{n+1} - \mathbf{x}_n)^\alpha - (\tilde{\mathbf{x}}_{n+1} - \mathbf{x}_n)^\alpha\| \leq C\varepsilon \|\mathbf{x}_{n+1} - \tilde{\mathbf{x}}_{n+1}\| \leq C(\varepsilon^3 h + \varepsilon^2 h^{k+1}),$$

leading to the error bound

$$\|\mathbf{v}^{[k, \mathbf{x}_n]}(t_{n+1}) - \tilde{\mathbf{v}}^{[k, \mathbf{x}_n]}(t_{n+1})\| \leq C(\varepsilon^3 h + \varepsilon^2 h^{k+1}). \quad (4.24)$$

Substituting (4.24) into (4.22) and following an analogous derivation of (4.23), we obtain $\|\mathbf{u}^{[k, \mathbf{x}_n]}(t_{n+1}) - \tilde{\mathbf{u}}^{[k, \mathbf{x}_n]}(t_{n+1})\| \leq C^2 \varepsilon^3 h^2 + C^2 \varepsilon^2 h^{k+2} + C\varepsilon h^{k+1}$, an improved estimate for $\mathbf{u}^{[k, \mathbf{x}_n]}$ compared to (4.23), which in turn yields an enhanced result $\|\mathbf{v}^{[k, \mathbf{x}_n]}(t_{n+1}) - \tilde{\mathbf{v}}^{[k, \mathbf{x}_n]}(t_{n+1})\| \leq C^2 \varepsilon^4 h^2 + C^2 \varepsilon^3 h^{k+2} + C\varepsilon^2 h^{k+1}$ for $\mathbf{v}^{[k, \mathbf{x}_n]}$ surpassing (4.24). Iterating this process, we derive for arbitrary m ,

$$\begin{aligned} \|\mathbf{u}^{[k, \mathbf{x}_n]}(t_{n+1}) - \tilde{\mathbf{u}}^{[k, \mathbf{x}_n]}(t_{n+1})\| &\leq C^m \varepsilon^{m+1} h^m + \sum_{l=1}^m C^l \varepsilon^l h^{k+l} = C^m \varepsilon^{m+1} h^m + \frac{C\varepsilon h^{k+1} (1 - C^m \varepsilon^m h^m)}{1 - C\varepsilon h}, \\ \|\mathbf{v}^{[k, \mathbf{x}_n]}(t_{n+1}) - \tilde{\mathbf{v}}^{[k, \mathbf{x}_n]}(t_{n+1})\| &\leq C^m \varepsilon^{m+2} h^m + \sum_{l=1}^m C^l \varepsilon^{l+1} h^{k+l} = C^m \varepsilon^{m+2} h^m + \frac{C\varepsilon^2 h^{k+1} (1 - C^m \varepsilon^m h^m)}{1 - C\varepsilon h}. \end{aligned}$$

Consequently, there exists a constant $\overline{h_0} < (C\varepsilon)^{-1}$ such that for $h < \overline{h_0}$, taking $m \rightarrow \infty$ yields the local estimate

$$\|\mathbf{x}^{[k, \mathbf{x}_n]}(t_{n+1}) - \tilde{\mathbf{x}}^{[k, \mathbf{x}_n]}(t_{n+1})\| \leq C\varepsilon h^{k+1}.$$

Global estimate. The procedure follows identically to Theorem 4.2 and is omitted here. \square

Remark 4.4. *The purpose of the iteration process in the local estimate is to handle potential zero eigenvalues induced by resonance. Our theorem results confirm that such resonances do not degrade the error estimates. When utilizing k -th order local linear extension variables and for any*

integer l satisfying $1 \leq l \leq k$, if the sum of any l eigenvalues of matrix A satisfies the condition $\lambda_{j_1} + \dots + \lambda_{j_l} = O(1)$, then Lemma 3.5 ensures that $A_1^{[k]}$ contains no zero eigenvalues. In this favorable scenario, the row-wise analytical framework on the first $k(d+1)+1$ matrix rows can be extended to all rows, thereby eliminating the specialized treatment of zero eigenvalues.

4.3. Application on second-order equations

Through the variable transformation $\mathbf{p} = \varepsilon \dot{\mathbf{y}}$ and denoting $\mathbf{u} = [\mathbf{y}^\top, \mathbf{p}^\top]^\top$, we reformulate the system (1.2) as a first-order differential equation in the form (1.1), where

$$A = \begin{bmatrix} \mathbf{0}_{d \times d} & I_d \\ -M & \mathbf{0}_{d \times d} \end{bmatrix}, \quad \mathbf{F}(\mathbf{u}, t) = \begin{bmatrix} \mathbf{0}_{d \times 1} \\ \varepsilon \mathbf{g}(\mathbf{y}, t) \end{bmatrix}, \quad \mathbf{x}_0 = \begin{bmatrix} \mathbf{y}_0 \\ \dot{\mathbf{y}}_0 \end{bmatrix}.$$

When M is a symmetric positive definite matrix, the matrix A is diagonalizable with its spectrum comprising d conjugate pairs of purely imaginary eigenvalues. Building upon the convergence results established in Theorems 4.2 and 4.3, we obtain the following high-order uniform convergence result.

Theorem 4.5. *Let $\mathbf{y}(t)$ and $\dot{\mathbf{y}}(t)$ be solutions of (1.2) that stay in a bounded domain independent of ε for $t \in [0, T]$. Suppose the derivatives of \mathbf{g} are Lipschitz continuous in both \mathbf{y} and t variables up to order k . Let $\rho = \max |\lambda(M)|$ and $\mu = \min |\lambda(M)|$. Then there exists a positive constant $h_0 < \frac{\pi \varepsilon}{2\sqrt{\rho}}$ such that for all $h < h_0$*

$$\|\mathbf{y}_n - \mathbf{y}(t_n)\| + \varepsilon \|\dot{\mathbf{y}}_n - \dot{\mathbf{y}}(t_n)\| \leq C \varepsilon h^{k+1}, \quad n = 0, \dots, T/h.$$

When $\nu \geq 1$, the bounded oscillatory energy condition is satisfied. Then there exist two positive constants $\underline{h}_0 > \frac{2\pi \varepsilon}{\sqrt{\mu}}$ and $\overline{h}_0 < (C\varepsilon)^{-1}$, such that for $\underline{h}_0 < h < \overline{h}_0$

$$\|\mathbf{y}_n - \mathbf{y}(t_n)\| + \varepsilon \|\dot{\mathbf{y}}_n - \dot{\mathbf{y}}(t_n)\| \leq C \varepsilon^2 h^k, \quad n = 0, \dots, T/h.$$

The constant C depends on A , T , k , \mathbf{y}_{in} , $\dot{\mathbf{y}}_{\text{in}}$ and the function \mathbf{g} , but is independent of h and ε .

5. Numerical results

This section presents some typical numerical experiments to confirm the optimality of the error bounds in Section 4. We denote the local linear extension exponential integrator using k -th order polynomials by LLEEI($k+1$). For more experiments, we refer to the work [60].

Example 1. The linear and nonlinear terms in (1.2) are chosen as $M = 1$ and $g(y, t) = -(t + \cos(2\sqrt{6}t)) \sin y$, respectively. The simulation is conducted up to the final time $T = 6$ with initial conditions $y(0) = \varepsilon$ and $\dot{y}(0) = \sqrt{3}$ to satisfy the bounded oscillatory energy condition. Since analytical solutions are unavailable for the numerical examples, reference solutions are obtained using the classical Runge-Kutta method of order four with a very small step size $h = 0.1/2^{18}$. The errors are measured by $\text{error}(\mathbf{y})$ and $\text{error}(\dot{\mathbf{y}})$, where $\text{error}(\cdot)$ denotes the global maximal error over the time steps $\{t_n\}_{n=0}^N$.

We first consider the weakly stiff regime by fixing $\varepsilon = 1/2^2$. The first row of Figure 1 displays the dependence of the numerical errors on the step size h . The vertical dotted line in each panel stands for $h = h_0$, where $h_0 = \frac{\pi\varepsilon}{2}$ is the threshold derived from Theorem 4.5 for this specific example. The results confirm that the LLEEI k methods show $(k+1)$ -th order convergence, indicating the arbitrarily high order convergence with increasing k . The absence of convergence for LLEEI5 and LLEEI6 in the panels is attributed to their numerical errors reaching machine precision. To examine convergence performance in the highly oscillatory regime, we select a representative parameter value $\varepsilon = 1/2^8$, with the results in the second row of Figure 1. Note that each panel contains two vertical dotted lines. From left to right, these lines correspond to the step sizes satisfying $h = h_0$ and $h = \underline{h}_0$, respectively, where \underline{h}_0 and h_0 are the theoretical thresholds introduced in Theorems 4.5. For this specific example, $\underline{h}_0 = 2\pi\varepsilon$. The results demonstrate that the k -th order convergence holds under the large step size condition $h > \underline{h}_0$, while the $(k+1)$ -th order convergence is achieved for $h < h_0$. Within the intermediate regime (h_0, \underline{h}_0) , the scheme retains both numerical stability and convergence.

Next, we investigate the uniformity of numerical errors across varying values of ε . The first row of Figure 2 presents the errors for various values of ε with a fixed small time step size $h = 1/2^6$. In each panel, two vertical dotted lines from left to right represent $\varepsilon = \underline{\varepsilon}_0$ and $\varepsilon = \varepsilon_0$. These thresholds take their values $\underline{\varepsilon}_0 = \frac{h}{2\pi}$ and $\varepsilon_0 = \frac{2h}{\pi}$, derived by solving the critical condition $h = \underline{h}_0 = \frac{2\pi\varepsilon}{\sqrt{\mu}}$ and $h = h_0 = \frac{\pi\varepsilon}{2\sqrt{\rho}}$ from Theorem 4.5 with the specific parameters used in this example, respectively. For cases where $\varepsilon > \varepsilon_0$ (or equivalently, $h < h_0$), the results demonstrate that the errors in \mathbf{y} for the LLEEI($k+1$) methods have the first-order dependence on ε , while the errors in $\dot{\mathbf{y}}$ are uniform. Finally, we consider a large step size $h = 1/2$, with the errors for different values of ε shown in the second row of Figure 2. The results confirm that for $\varepsilon < \underline{\varepsilon}_0$ (or equivalently, $h > \underline{h}_0$), the numerical solutions for \mathbf{y} and $\dot{\mathbf{y}}$ exhibit second-order and first-order convergence with respect to

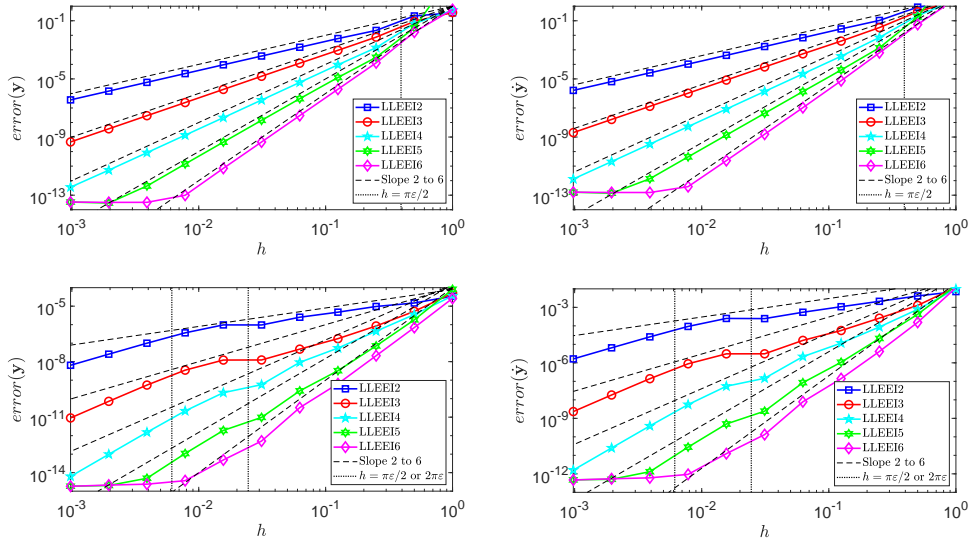


Figure 1: Error versus step size h . The first row corresponds to the weakly oscillatory case ($\epsilon = 1/2^2$), while the second row represents the highly oscillatory regime ($\epsilon = 1/2^8$). The left and right columns display the numerical errors for y and \dot{y} , respectively.

ε , respectively, consistent with the predictions of Theorem 4.5. Within the range $\varepsilon \in (\underline{\varepsilon}_0, \varepsilon_0)$ (or equivalently, $h \in (h_0, \underline{h}_0)$), the LLEEI methods preserve ε -uniform accuracy.

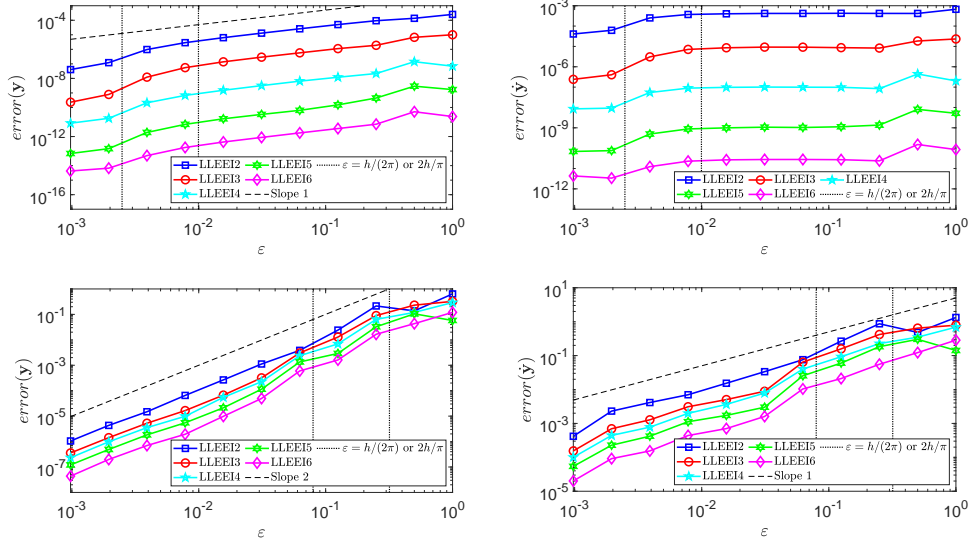


Figure 2: Error versus step size ε . The first row corresponds to the small step size case ($h = 1/2^6$), while the second row represents the large step size case ($h = 1/2$). The left and right columns display the numerical errors for \mathbf{y} and $\dot{\mathbf{y}}$, respectively.

Example 2. We consider the system (1.1) specified with the following matrix and nonlinear function

$$A = \begin{bmatrix} 0 & 0 & 1 & 0 \\ 0 & 0 & 0 & 1 \\ E & 0 & 0 & B \\ 0 & E & -B & 0 \end{bmatrix}, \quad \mathbf{F} = \begin{bmatrix} 0 \\ 0 \\ g_1(\mathbf{u}) \\ g_2(\mathbf{u}) \end{bmatrix}, \quad (5.1)$$

which models the 2D charged particle dynamics in an isotropic strong electric field and a perpendicular homogeneous strong magnetic field. Through the scaling $\mathbf{p} = \varepsilon \dot{\mathbf{y}}$, this system, with the state variable defined as $\mathbf{u} = [\mathbf{y}^\top, \mathbf{p}^\top]^\top$, is transformed from the underlying second-order equation

$$\ddot{\mathbf{y}} = \frac{E}{\varepsilon^2} \mathbf{y} + \frac{B}{\varepsilon} J \dot{\mathbf{y}} + \frac{1}{\varepsilon} \mathbf{g}(\mathbf{y}, t), \quad J = \begin{bmatrix} 0 & 1 \\ -1 & 0 \end{bmatrix},$$

where E and B denote the electric and magnetic field intensities, respectively. We set $\mathbf{y}(0) = [0, 0]^\top$,

the particle emission from the origin with velocity $\dot{\mathbf{y}}(0) = [3, 4]^\top$ for the initial conditions. The magnetic field is set by $B = 1$, and the nonlinear term is given by the electrostatic force

$$\mathbf{g}(\mathbf{y}, t) = \begin{bmatrix} \frac{y_1}{(y_1^2 + y_2^2 + (2 - \cos(\pi t))^2)^{\frac{3}{2}}} \\ \frac{y_2}{(y_1^2 + y_2^2 + (2 - \cos(\pi t))^2)^{\frac{3}{2}}} \end{bmatrix}.$$

We consider two configurations, $E = 6$ and $E = 3$, for the electric field. In the first case ($E = 6$), the matrix A in (5.1) possesses eigenvalues $\lambda(A) = \{\pm 2i, \pm 3i\}$, where the corresponding high-frequency oscillators determined by the linear part share a common period. The second case ($E = 3$) produces eigenvalues $\lambda(A) = \left\{ \pm \sqrt{\frac{7 \pm \sqrt{13}}{2}} i \right\}$, resulting in non-resonant oscillators.

For comparison in the following experiments, we consider the second and third-order exponential time differencing Runge-Kutta methods from [29], along with the fourth-order method from [31], labelled as ETDRK2, ETDRK3, and ETDRK4, respectively. We also consider the k -th order exponential Rosenbrock methods from [30], denoted by EXPRB k . We remark that EXPRB2 is fundamentally equivalent to LLEEI2 [60]. Classical Runge-Kutta methods of order k are referred to as RK k . We directly implement the LLEEI methods, requiring neither the diagonalization of A in advance nor any preprocessing of periodic effects. Figure 3 shows the error dependence of \mathbf{u} on step size h with fixed $\varepsilon = 1/2^2$ and $\varepsilon = 1/2^8$, respectively. In weakly oscillatory regimes, panels in the first row of Figure 3 show that all methods attain theoretical convergence rates, with only minor performance variations among exponential-type methods. For highly oscillatory cases, the numerical results in the second row demonstrate that the LLEEI methods show the same piecewise convergence behavior, in complete agreement with the theoretical results in Theorems 4.2 and 4.3. ETDRK and EXPRB methods maintain stability for stiffness, yet their convergence is limited by the oscillatory characteristics of the solution. The Runge-Kutta methods exhibit instability in these cases, thus their resulting curves are omitted. We further observe that whether the eigenvalues of matrix A are integer multiples of a common frequency shows negligible influence on the performance of exponential-type methods.

Figure 4 depicts the error variation with respect to ε under two step sizes $h = 1/2^3$ and $h = 1/2^8$, respectively. The results clearly demonstrate that only the LLEEI methods preserve ε -uniform accuracy under the small step size condition (panels in the second row), whereas the errors of all other tested schemes grow as ε decreases. The large step size scenario (panels in the first row) also demonstrates that the error of the LLEEI methods decreases consistently as ε decreases. The

second row of Figure 3, along with Figure 4, highlights that the accuracy behavior of LLEEs outperforms conventional EIs across all tested step sizes in highly oscillatory regimes due to their uniform accuracy property, with the advantage becoming more pronounced as the method order increases.

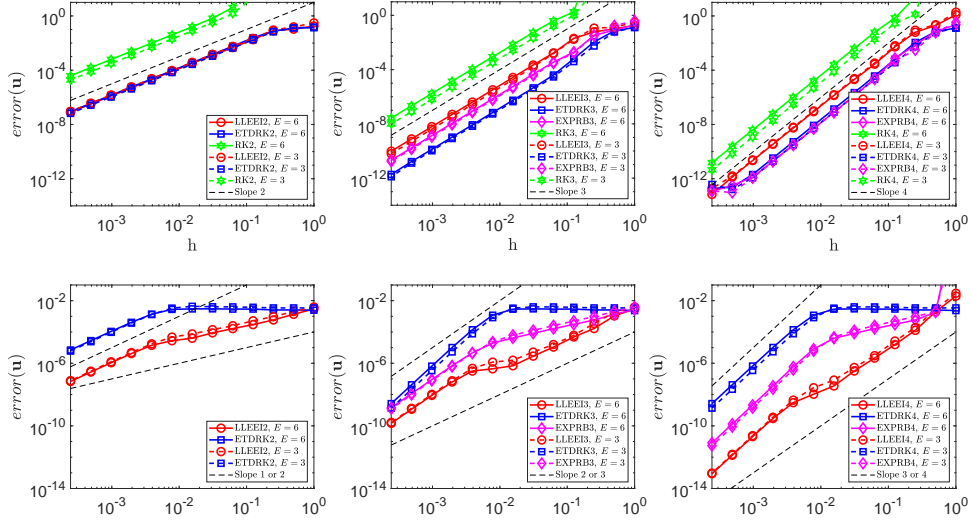


Figure 3: $\text{error}(\mathbf{u})$ versus step size h . The first row corresponds to the weakly oscillatory case ($\epsilon = 1/2^2$), while the second row represents the highly oscillatory regime ($\epsilon = 1/2^8$). The left, middle, and right columns correspond to second-, third-, and fourth-order methods, respectively.

6. Conclusion

This paper develops a rigorous theoretical framework for local linear extension exponential integrators applied to highly oscillatory ODEs. We first present a systematic review of the construction of local linear extension variables and their associated systems, followed by the derivation of the new class of EIs. Through introducing tensor product structures and performing precise algebraic operations, we demonstrate that the linear part of the high-dimensional extension system preserves essential spectral properties, including eigenvalue characteristics and diagonalizability. Some specific invariant subspaces of the differential operator and their matrix representations are analysed. These fundamental algebraic properties validate the effectiveness of the dimension-raising

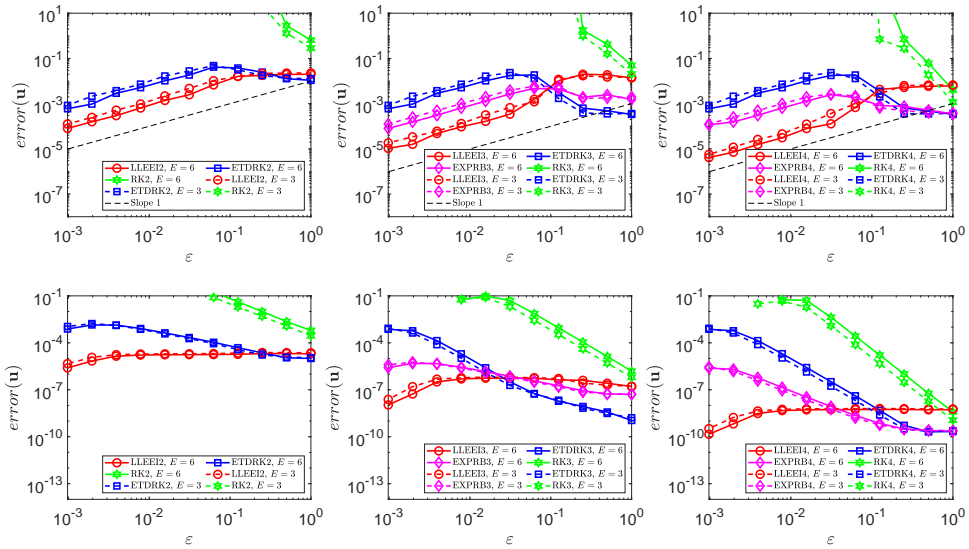


Figure 4: $\text{error}(\mathbf{u})$ versus ε . The first row corresponds to the large step size case ($h = 1/2^3$), while the second row represents the small step size case ($h = 1/2^8$). The left, middle, and right columns correspond to second-, third-, and fourth-order methods, respectively.

approach and further provide the theoretical basis for proving the uniform accuracy of the numerical schemes. The analysis establishes convergence results across different parameter regimes. When solving highly oscillatory systems using large time steps $h > C\varepsilon$, some key elements play pivotal roles: the adiabatic transformation technique, the periodic decomposition method, and the superior algebraic properties of the local linear extension system. These allow separate analysis of oscillatory and non-oscillatory components. The numerical approach naturally yields solutions with improved uniform accuracy with respect to ε for second-order non-autonomous equations. Numerical experiments confirm the optimality of these theoretical results.

Acknowledgement

This work was supported by the National Key R&D Program of China (2024YFA1012600) and the NSFC grant 12171237.

References

- [1] K. Lorenz, T. Jahnke, C. Lubich, Adiabatic integrators for highly oscillatory second-order linear differential equations with time-varying eigendecomposition, *Bit Numerical Mathematics* 45 (1) (2005) 91–115.
- [2] J. M. Franco, New methods for oscillatory systems based on ARKN methods, *Applied Numerical Mathematics* 56 (8) (2006) 1040–1053.
- [3] X. Y. Wu, X. O. You, W. Shi, B. Wang, ERKN integrators for systems of oscillatory second-order differential equations, *Computer Physics Communications* 181 (11) (2010) 1873–1887.
- [4] M. P. Calvo, P. Chartier, A. Murua, J. M. Sanz-Serna, A stroboscopic numerical method for highly oscillatory problems, in: *Workshop on Numerical Analysis and Multiscale Computations*, Vol. 82 of *Lecture Notes in Computational Science and Engineering*, 2012, pp. 71–+.
- [5] E. Hairer, C. Lubich, G. Wanner, *Geometric Numerical Integration: Structure-Preserving Algorithms for Ordinary Differential Equations*, Springer Series in Computational Mathematics, Springer Berlin Heidelberg, 2013.

- [6] N. Crouseilles, M. Lemou, F. Mehats, X. F. Zhao, Uniformly accurate Particle-in-Cell method for the long time solution of the two-dimensional Vlasov-Poisson equation with uniform strong magnetic field, *Journal of Computational Physics* 346 (2017) 172–190.
- [7] D. Cohen, T. Jahnke, K. Lorenz, C. Lubich, Numerical integrators for highly oscillatory Hamiltonian systems: A review, in: A. Mielke (Ed.), *Analysis, Modeling and Simulation of Multiscale Problems*, Springer Berlin Heidelberg, Berlin, Heidelberg, 2006, pp. 553–576.
- [8] B. García-Archilla, J. M. Sanz-Serna, R. D. Skeel, Long-time-step methods for oscillatory differential equations, *SIAM Journal on Scientific Computing* 20 (3) (1998) 930–963.
- [9] E. Hairer, C. Lubich, Long-time energy conservation of numerical methods for oscillatory differential equations, *Siam Journal on Numerical Analysis* 38 (2) (2000) 414–441.
- [10] X. Wu, X. You, B. Wang, *Structure-Preserving Algorithms for Oscillatory Differential Equations*, Springer Berlin, Heidelberg, 2013.
- [11] B. Leimkuhler, S. Reich, *Simulating Hamiltonian dynamics*, Cambridge university press, 2004.
- [12] K. Feng, M. Qin, *Symplectic geometric algorithms for Hamiltonian systems*, Vol. 449, Springer, 2010.
- [13] X. F. Zhao, Uniformly accurate multiscale time integrators for second order oscillatory differential equations with large initial data, *Bit Numerical Mathematics* 57 (3) (2017) 649–683.
- [14] W. Bao, X. Dong, X. Zhao, Uniformly accurate multiscale time integrators for highly oscillatory second order differential equations, *Journal of Mathematical Study* 47 (2) (2014) 111–150.
- [15] B. Wang, Y. L. Jiang, Improved uniform error bounds on parareal exponential algorithm for highly oscillatory systems, *Bit Numerical Mathematics* 64 (1) (2024).
- [16] Y. Y. Cai, Y. C. Guo, Uniformly accurate nested Picard integrators for a system of oscillatory ordinary differential equations, *Bit Numerical Mathematics* 61 (4) (2021) 1115–1152.
- [17] W. Gautschi, Numerical integration of ordinary differential equations based on trigonometric polynomials, *Numerische Mathematik* 3 (1961) 381–397.

- [18] M. Hochbruck, C. Lubich, A Gautschi-type method for oscillatory second-order differential equations, *Numerische Mathematik* 83 (3) (1999) 403–426.
- [19] V. Grimm, On error bounds for the Gautschi-type exponential integrator applied to oscillatory second-order differential equations, *Numerische Mathematik* 100 (2005) 71–89.
- [20] V. Grimm, M. Hochbruck, Error analysis of exponential integrators for oscillatory second-order differential equations, *Journal of Physics A-Mathematical and General* 39 (19) (2006) 5495–5507.
- [21] D. Cohen, E. Hairer, C. Lubich, Modulated Fourier expansions of highly oscillatory differential equations, *Foundations of Computational Mathematics* 3 (2003) 327–345.
- [22] D. Cohen, E. Hairer, C. Lubich, Numerical energy conservation for multi-frequency oscillatory differential equations, *BIT Numerical Mathematics* 45 (2005) 287–305.
- [23] D. Cohen, Conservation properties of numerical integrators for highly oscillatory Hamiltonian systems, *IMA Journal of numerical analysis* 26 (1) (2006) 34–59.
- [24] E. Hairer, C. Lubich, B. Wang, A filtered Boris algorithm for charged-particle dynamics in a strong magnetic field, *Numerische Mathematik* 144 (4) (2020) 787–809.
- [25] B. Wang, X. F. Zhao, Geometric two-scale integrators for highly oscillatory system: Uniform accuracy and conservations, *Siam Journal on Numerical Analysis* 61 (3) (2023) 1246–1277.
- [26] B. Wang, X. Y. Wu, J. L. Xia, Error bounds for explicit ERKN integrators for systems of multi-frequency oscillatory second-order differential equations, *Applied Numerical Mathematics* 74 (2013) 17–34.
- [27] B. Wang, X. Y. Wu, F. W. Meng, Trigonometric collocation methods based on Lagrange basis polynomials for multi-frequency oscillatory second-order differential equations, *Journal of Computational and Applied Mathematics* 313 (2017) 185–201.
- [28] J. Cui, Z. Xu, Y. Wang, C. Jiang, Mass- and energy-preserving exponential Runge–Kutta methods for the nonlinear Schrödinger equation, *Applied Mathematics Letters* 112 (2021) 106770.

- [29] S. M. Cox, P. C. Matthews, Exponential time differencing for stiff systems, *Journal of Computational Physics* 176 (2) (2002) 430–455.
- [30] M. Hochbruck, A. Ostermann, J. Schweitzer, Exponential Rosenbrock-type methods, *Siam Journal on Numerical Analysis* 47 (1) (2009) 786–803.
- [31] S. Krogstad, Generalized integrating factor methods for stiff PDEs, *Journal of Computational Physics* 203 (1) (2005) 72–88.
- [32] A. Tokman, Efficient integration of large stiff systems of odes with exponential propagation iterative (EPI) methods, *Journal of Computational Physics* 213 (2) (2006) 748–776.
- [33] E. Celledoni, D. Cohen, B. Owren, Symmetric exponential integrators with an application to the cubic Schrödinger equation, *Foundations of Computational Mathematics* 8 (2008) 303–317.
- [34] L. Mei, X. Wu, Symplectic exponential Runge–Kutta methods for solving nonlinear Hamiltonian systems, *Journal of Computational Physics* 338 (2017) 567–584.
- [35] M. Hochbruck, A. Ostermann, Exponential integrators, *Acta Numerica* 19 (2010) 209–286.
- [36] B. Wang, K. Liu, X. Wu, A filon-type asymptotic approach to solving highly oscillatory second-order initial value problems, *Journal of Computational Physics* 243 (2013) 210–223.
- [37] M. Khanamiryan, Quadrature methods for highly oscillatory linear and nonlinear systems of ordinary differential equations: part I, *Bit Numerical Mathematics* 48 (4) (2008) 743–761.
- [38] H. De la Cruz, R. J. Biscay, F. Carbonell, T. Ozaki, J. C. Jimenez, A higher order local linearization method for solving ordinary differential equations, *Applied Mathematics and Computation* 185 (1) (2007) 197–212.
- [39] A. Koskela, A. Ostermann, Exponential Taylor methods: Analysis and implementation, *Computers & Mathematics with Applications* 65 (3) (2013) 487–499.
- [40] J. I. Ramos, C. M. GarciaLopez, Piecewise-linearized methods for initial-value problems, *Applied Mathematics and Computation* 82 (2-3) (1997) 273–302.
- [41] M. Caliari, A. Ostermann, Implementation of exponential Rosenbrock-type integrators, *Applied Numerical Mathematics* 59 (3-4) (2009) 568–581.

[42] D. Li, X. Li, Relaxation exponential Rosenbrock-type methods for oscillatory Hamiltonian systems, *SIAM Journal on Scientific Computing* 45 (6) (2023) A2886–A2911.

[43] E. Weinan, Analysis of the heterogeneous multiscale method for ordinary differential equations, *Communications in Mathematical Sciences* 1 (3) (2003) 423–436.

[44] A. Abdulle, E. Weinan, B. Engquist, E. Vanden-Eijnden, The heterogeneous multiscale method, *Acta Numerica* 21 (2012) 1–87.

[45] W. E, B. Engquist, X. T. Li, W. Q. Ren, E. Vanden-Eijnden, Heterogeneous multiscale methods: A review, *Communications in Computational Physics* 2 (3) (2007) 367–450.

[46] M. P. Calvo, J. M. Sanz-Serna, Heterogeneous multiscale methods for mechanical systems with vibrations, *Siam Journal on Scientific Computing* 32 (4) (2010) 2029–2046.

[47] G. Ariel, B. Engquist, S. Kim, Y. Lee, R. Tsai, A multiscale method for highly oscillatory dynamical systems using a Poincaré map type technique, *Journal of Scientific Computing* 54 (2013) 247–268.

[48] P. Chartier, J. Makazaga, A. Murua, G. Vilmart, Multi-revolution composition methods for highly oscillatory differential equations, *Numerische Mathematik* 128 (1) (2014) 167–192.

[49] P. Chartier, N. Crouseilles, X. F. Zhao, Numerical methods for the two-dimensional Vlasov-Poisson equation in the finite Larmor radius approximation regime, *Journal of Computational Physics* 375 (2018) 619–640.

[50] P. Chartier, M. Lemou, F. Mehats, G. Vilmart, A new class of uniformly accurate numerical schemes for highly oscillatory evolution equations, *Foundations of Computational Mathematics* 20 (1) (2020) 1–33.

[51] P. Chartier, N. J. Mauser, F. Méhats, Y. Zhang, Solving highly-oscillatory NLS with SAM: Numerical efficiency and long-time behavior, *Discrete and Continuous Dynamical Systems-Series S* 9 (5) (2016) 1327–1349.

[52] F. Castella, P. Chartier, F. Méhats, A. Murua, Stroboscopic averaging for the nonlinear Schrödinger equation, *Foundations of Computational Mathematics* 15 (2) (2015) 519–559.

[53] W. Bao, Y. Cai, X. Jia, Q. Tang, A uniformly accurate multiscale time integrator pseudospectral method for the Dirac equation in the nonrelativistic limit regime, *SIAM Journal on Numerical Analysis* 54 (3) (2016) 1785–1812.

[54] W. Bao, Y. Cai, Uniform and optimal error estimates of an exponential wave integrator sine pseudospectral method for the nonlinear Schrödinger equation with wave operator, *SIAM Journal on Numerical Analysis* 52 (3) (2014) 1103–1127.

[55] Y. Feng, Z. Xu, J. Yin, Uniform error bounds of exponential wave integrator methods for the long-time dynamics of the dirac equation with small potentials, *Applied Numerical Mathematics* 172 (2022) 50–66.

[56] Y. Feng, W. Yi, Uniform error bounds of an exponential wave integrator for the long-time dynamics of the nonlinear Klein–Gordon equation, *Multiscale Modeling & Simulation* 19 (3) (2021) 1212–1235.

[57] S. Baumstark, E. Faou, K. Schratz, Uniformly accurate exponential-type integrators for Klein–Gordon equations with asymptotic convergence to the classical NLS splitting, *Mathematics of Computation* 87 (311) (2018) 1227–1254.

[58] Y. Cai, X. Zhou, Uniformly accurate nested Picard iterative integrators for the Klein–Gordon equation in the nonrelativistic regime, *Journal of Scientific Computing* 92 (2) (AUG 2022).

[59] P. Chartier, N. Crouseilles, M. Lemou, F. Méhats, Uniformly accurate numerical schemes for highly oscillatory Klein–Gordon and nonlinear Schrödinger equations, *Numerische Mathematik* 129 (2015) 211–250.

[60] Z. Qi, W. Deng, A novel class of exponential integrators for highly oscillatory second-order differential equations with uniform accuracy, *Preprint* (2025).

[61] T. Jahnke, Long-time-step integrators for almost-adiabatic quantum dynamics, *SIAM Journal on Scientific Computing* 25 (6) (2004) 2145–2164.

[62] N. J. Higham, *Functions of Matrices*, Society for Industrial and Applied Mathematics, 2008.